STRUCTURAL ANALYSIS OF Ge NANOPARTICLES EMBEDDED ZnO THIN FILMS BY LASER INDUCED BREAKDOWN SPECTROSCOPY

Ge NANOPARÇACIK KATKILI ZnO İNCE FİLMLERİN LAZER ETKİLİ BOZULMA SPEKTROSKOPİSİ İLE YAPISAL ANALİZİ

MEHMET SİNAN TOPCU

DOÇ. DR. ABDULLAH CEYLAN
Supervisor

Submitted to Graduate School of Science and Engineering of Hacettepe University
As a Partial Fulfillment to the Requirements
For the Award of the Degree of Master of Philosophy
in Physics

2016

This work named "**Structural analysis of Ge nanoparticles embedded ZnO thin films by Laser Induced Breakdown Spectroscopy (LIBS)**" by **MEHMET SİNAN TOPCU** has been approved as a thesis for the Degree of **MASTER OF PHILOSOPHY IN PHYSICS** by the below mentioned Examining Committee Members

Prof. Dr. Şadan ÖZCAN
Head .....

Assoc. Prof. Dr. Abdullah CEYLAN
Supervisor .....

Asst. Prof. Dr. Kemal Efe ESELLER
Member .....

This thesis has been approved as a thesis for the Degree of **MASTER OF SCIENCE IN PHILOSOPHY** by Board of Directors of the Institute for Graduate School of Science and Engineering

Prof. Dr. Salih Bülent ALTEN
Director of the Institute of
Graduate School of Science and Engineering

DEDICATION

I would like to dedicate this thesis to my doughter: Ece Topcu and my wife: Pelin Bagdas Topcu.

ETHICS

In this thesis study, prepared in accordance with the spelling rules of Institute of Graduate Studies in Science of Hacettepe University,

I declare that

- all the information and documents have been obtained in the base of the academic rules
- all audio-visual and written information and results have been presented according to the rules of science ethics
- in case of using other Works, related studies have been cited in accordance with the scientific standards
- all cited studies have been fully referenced
- I did not do any distortion in the data set
- and any part of this thesis has not been presented as another thesis study at this or any other university.

29/07/2016

MEHMET SİNAN TOPCU

ÖZET

Ge Nanoparçacık Katkılı ZnO İnce Filmlerin Lazer Etkili Bozulma Spektroskopisi İle Yapısal Analizi

M. Sinan TOPCU

Yüksek Lisans, Fizik Mühendisliği Anabilim Dalı

Tez Danışmanı: Doç. Dr. Abdullah CEYLAN

Temmuz 2016, 64 sayfa

Lazer etkili bozulma spektroskopisi (LIBS), Ge (Ge-np) nanoparçacık katkılanmış ZnO çoklu katmanlı ince filmlerin büyük ölçekli yapısal araştırması için kullanıldı. Bu çalışmanın nihai gayesi, LIBS tekniğinin nano kompozit ince film yapılarının in-situ analizi için uygunluğunu, XRD ve SEM gibi başka tekniklerin sonuçları ile karşılaştırarak saptamaktı. (Ge-np) içeren ZnO ince filmler yeni opto-elektronik cihazlarda uygulanabilirlik potansiyelleri sebebiyle hatırı sayılır derecede dikkat çekmiştir. Geniş Bohr yarıçapına sahip Ge, yaklaşık 24 nm, üretim kolaylığıda düşünüldüğünde, dahada ilginç hale getirmektedir. Bu yüzden, opto-elektronik özellikleri ile yapısı arasında korelasyon yapabilmek için ZnO:Ge yapısını tümüyle araştırmak önemlidir. LIBS, araştırılan örneğin atomları ile plasma oluşturan, temel spektroskopik in-situ analiz metodudur. Bu sebeple LIBS, 100 – 200 nm derinlikteki parçacıkları, derinlik profilleme ile analiz etmek için kullanılabilir ve sonuç olarak homojenite tayini yapılabilir. Hızlı, tekrarlanabilir, düşük maliyetli ve minimum örnek hazırlama analizi, Ge nanoparçacıkları belirlemek için uygulandı. ZnO:Ge ince filmlerin yapısal analizini yapmak maksadı ile, LIBS sistemi, örnekleme metodlarına karşı maksimum spektrum şiddeti ile uygulandı. Ardışık püskürtme ve ardışık hızlı termal tavlama (RTA) yöntemleri ile Si alttaş üzerine kaplanmış ZnO ve Ge tabakaları ile oluşturulmuş ZnO:Ge ince filmlerin yapısı birkaç dakika içinde tanımlandı. Sonuçlar, SEM, SIMS ve XRD sonuçları ile karşılaştırıldı. Sonunda, en iyi tayin şartlarını sağlamak için, sinyal gürültü oranı (SNR) ve relatif standart

sapma (RSDT) hesaplandı. Türlerin belirgin spektrumları, LIBS'in nano parçacık katkılı ince film aplikasyonlarında ümit verici bir, yapısal oluşum ve homojenlik analizi tekniği olduğunu gösteriyor.

Anahtar Kelimeler: ZnO:Ge İnce filmler, LIBS, yapısal analiz, atomic spektrum, ince filmlerin kalınlık profili, homojenlik araştırması.

ABSTRACT

Structural analysis of Ge nanoparticles embedded ZnO thin films by Laser Induced Breakdown Spectroscopy (LIBS)

M. Sinan TOPCU

Master of Philosophy, Department of Physics Engineering

Supervisor: Assoc. Prof. Abdullah CEYLAN

July 2016, 64 pages

Laser Induced Breakdown Spectroscopy (LIBS) is employed for the wide scale structural investigation of Ge nanoparticles (Ge-np) embedded multilayered ZnO thin films. The ultimate goal of this study was to determine if LIBS technique is suitable for in-situ analysis of nano composite thin film structures by comparing the results of other techniques like XRD and SEM. ZnO thin films including (Ge-np) have attracted a considerable attention due to their potential applicability on new opto-electronic devices. Ge having a larger Bohr radius, which is about 24 nm, makes it more interesting as far as the production easiness is concerned. Hence, it is important to thoroughly investigate the ZnO:Ge structure for making correlation between opto-electronic properties and the structure. LIBS is a elemental spectrometric in-situ analyses method, with causing a plasma with the atoms of the sample investigated. Therefore LIBS can be used to analyze the particles in 100-200 nm depth by means of depth profiling and as a result, homogeneity of sample can be determined. Fast and reproducible, low cost, with minimum sample preparation analysis was implemented to identify the Ge nanoparticles. With the purpose of making the structural analyses of ZnO:Ge thinfilms, LIBS system was implemented with maximum spectrum intensity versus sampling methods. Structure of ZnO:Ge thin films produced on substrates of Si by sequential sputtering and subsequent rapid thermal annealing of sputtered ZnO and Ge layers were identified within couple of minutes under ambient conditions. Results were compared with SEM, SIMS and XRD results.

Eventually, signal to noise (SNR) and relative standard deviation (RSDT) have been calculated to maintain the best detection conditions. Distinct spectra of specimens shows LIBS as a promising technique for analyzing the formation structure and homogeneity of nano particle embedded thin film applications.

Keywords: ZnO:Ge thinfilms, LIBS, structural analyses, atomic spectrum, depth profile of thinfilms, homogeneity investigation

ACKNOWLEDGEMENTS

I would like to thank my advisor Assoc. Dr. Abdullah Ceylan for his endless support during my graduate studies at Hacettepe University. I'm very pleased to thank Dr. K. Efe Eseller for guidance in this thesis. I would like to thank my committee member Prof Dr. Şadan Özcan for his great encouraging way of support. I would like to thank Prof. Dr. İsmail Hakkı Boyacı, Banu Sezer and Gonca Bilge for their valuable support during data collection of this thesis. I would like also to thank Deniz Çalışkan (Nanotam, Bilkent Nanotechnology Research Center) for his friendly and supportive help for supplying crucial data used in this thesis. Finally I would like to thank my family for encouraging me in this graduate study.

TABLE OF CONTENTS

Page

SYMBOLS AND ABBREVIATIONS

Symbols

Ψ	Wave function
A_{nm}	Einstein emission coefficient
τ	Life time
h	Planck constant
$\Delta\nu$	Spectral line broadening
μ	Magnetic dipole

Abbreviations

LIBS	Laser induced breakdown spectroscopy
LSS	Laser spark spectroscopy
LOES	Laser optical emission spectroscopy
EMR	Electromagnetic emission
Nd:YAG	Neodymium-doped yttrium aluminum garnet
XeCl	Xenon monochloride
KrF	Krypton fluoride
ArF	Argon fluoride
CO_2	Carbon dioxide
UV	Ultraviolet
IR	Infrared
FOC	Fiber optic cable
OH	Oxygen monoxide
n	Refractive index
CCD	Charge coupled device

ICCD	Intense charge coupled device
PMT	Photo multiplier tube
CID	Coupled injection device
CTD	Charge transfer device
MOS	Metal oxide semiconductor
PDA	Photo diode array
MCP	Micro channel plate
Si	Silicon
Ge	Germanium
Zn	Zinc
Ca	Calcium
ZnO	Zinc oxide
RTA	Rapid thermal annealing
SNR	Signal to noise ratio
STD	Standard deviation
RSTD	Relative standard deviation

1. INTRODUCTION

It is known that quantum confinement effect in semiconducting materials leads to significant change in electronic and band structures, so that semiconducting produced having pronounced changes in optical and electrical properties. There are so many studies on Ge nanocrystals embedded Si structures with promisingly wide band gap. Ge element which is having a larger Bohr radius of about 24nm when compared to Si which is about 5nm is making a significant quantum confinement effect.[1], [2], [3], [4], [5], [6]. In light of this knowledge, other embedding medium was utilized in the current literature as ZnO with a very promising candidate for photovoltaic applications [7], [8]. ZnO when corresponded to other wide gap materials such as ZnSe and GaN has better features because of larger exciton binding energy approximately 60 meV. Ge nanoparticles embedded ZnO medium (ZnO:Ge structure) was studied with different type of structural analyses techniques as X-Ray Diffraction (XRD), Secondary Ion Mass Spectroscopy (SIMS) and Scanning Electron Microscopy (SEM) [9], and resulted with different informations of the structure. We investigated the same structure with a significantly easy and fast method of structural analyses called Laser Induced Breakdown Spectroscopy (LIBS). (LIBS) method of elemental analyses is advantageous when compared to other methods in fast and contactless data collection, no long and onerous process for sample preparation, no need for vacuum conditions and no need to use any reactive chemicals for fulfilling some observation criteria. In literature 2D surface analyses performed with LIBS in Ge embedded SiO_2 and it is proved that LIBS is a promising and fast method for semi-quantitative analyses of investigated element for thin film structures [10]. In light of the studies performed, 2D homogeneity mapping is performed for Ge embedded ZnO structure which is uniquely processed as will be described in detail in the theoretical background chapter of this study. This is also a distinctive study as the results will be compared with other conventional structural analyses methods (XRD and SEM). Four different type processed, ZnO:Ge matrix (annealed for different durations) are analyzed to compare the different matrix formations of samples with each other as well.

(LIBS) Laser induced breakdown spectroscopy is a method of atomic emission spectroscopy. System consists of a high energy laser source. Laser produces high energy laser pulse beam and evaporates the small sized particles on the sample. Thus created high temperature spark dissociates the sample into neutral and ionic atoms and causing a plasma

state of the particles plucked from the sample. Plasma created on the surface is directed to a spectrometer via a collective lens. Element concentration in the investigated sample is directly depended to the intensity of the spectrum observed from that element. LIBS signal can be detected after micro second of plasma formation and the measurement can be done independent from time and space. After 0.1 μs of plasma formation, ionic emission from the elements is observed and then the atomic emission observed.

It is possible to perform analyses of the sample independent from it is physical phase, as because in sufficient high temperatures all elements have characteristic emission frequencies. All elements can be analyzed according to the power of the laser, sensitivity of the spectrometer and the wavelength band.

Working principle of LIBS is demonstrated in Figure 1.1

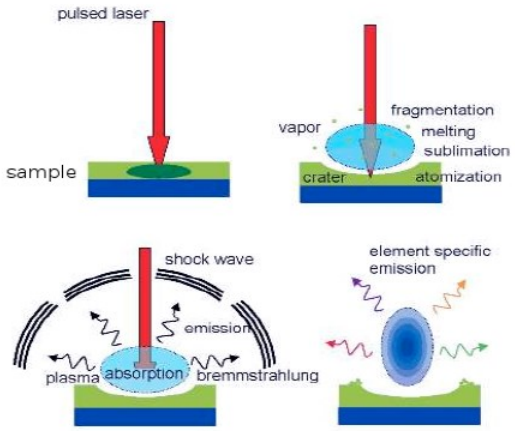

Figure 1.1 Illustration of LIBS

LIBS is used in geology, space, medical, archeology, military, crime and industrial areas and applications. In metallurgy it is used for soil and mineral analyses. In space sciences it is used to understand the composition of the surface of Mars so the conditions and the properties of the medium. In environmental sciences to determine the quality of air and water. In medical sciences to find the mutated living cell caused by cancer, to find the heavy metal toxicities from hair and teeth samples, to specify the viruses, allergy sources, mold spores. In archeology to determine the quality of restoration. In military to find the biological weapons, explosives. In industry to describe the contamination and ingredients of the material.

Although, LIBS is used in many different analyses examples, it is not a sensitive measurement, has low measurement accuracy and hard to work with liquid samples. Laser pulse energy is differing from shot to shot so the obtained emission intensities are differing from shot to shot.

The objective is to setup a fast and easy method of determining the homogeneity of multilayer thin film solar cells.

In this study we compared the depth profiling figures obtained by profiler and the consecutive shot intensities derived from LIBS data to figure out the film thickness, which will also give crucial information on the thin film formation process deviations and errors with a fast and reliable method?

Comparing the known and verified results of other type of structural analyses methods for ZnO:Ge thin films (mentioned above) and to introduce the LIBS as a promising structural analyzing method with its specific advantages is another objective of this study.

2. Theoretical Background

2.1 Atomic Emission Spectroscopy

Atoms have translational and electronic states also have spin and nuclear spins. On the other hand molecules have vibrational and rotational structures. Atoms nucleus is positively charged and bounded to the negatively charged electrons with electrostatic forces. Atomic spectra are defined by the wavelength, intensity of the intrinsic line in spectra and the line series, depending on the characteristic of the line. Electromagnetic radiation emitted by the bound – bound transitions are discontinuous which means are isolated wavelengths. One can identify atomic structure by energy level. Ballmer showed a relation which is representing the wavelengths of hydrogen atomic spectrum lines. Quantum structure of atoms is proving quantum mechanical behavior of atoms which is stated in Bohr postulates that are having discrete energy levels. Emission or absorption of radiation occurs when an electron moves from an energy level to another one. Spectral lines with fine and hyperfine structure demonstrates the theoretical structure of atomic spectroscopy. Line broadening of the spectral lines is categorized in groups according to the phenomena acting on the spectrum. Which can be described as, Doppler Broadening resulting from translational broadening, Pressure Broadening from collisions, Stark Broadening from the presence of electric field and Zeeman Effect from presence of magnetic field.

2.1.1 Atomic Structure

Structure of atoms was explained with electrostatic approach at the beginning. According to this approach attractive and repulsive forces between nucleus and electrons due to electrostatic forces forms the atoms. However this way of modeling the structure of an atom is not sufficient and complete to describe the real structural model of the atom. In order describe and understand the electron orbital's in more detail one should investigate the quantum mechanical approach. In this approach Schrödinger equation gives atoms a wave function Ψ which has n, l and m quantum numbers. The principal quantum number "n" is 1,2,3,… with electron orbital quantum number l which is = 0,1,2,3,4,… and shown with s,p,d,f,g,h,… . Pauli Exclusion Principle says that electrons cannot occupy the same energy level with the same group of quantum numbers n, l, m_l and m_s where the last two are magnetic angular and magnetic spin numbers accordingly. Each orbital can have 2 (2l

+ 1) m_l quantum numbers. According to this minimum of 2 electrons can occupy "ns" orbital while max of 6 electrons can occupy the "np" orbital. Electron spin angular quantum number "s" is related with the electron spin quantum number m_s that only have the values of ± ½ . Derived from here it is obvious that total angular momentum of an electron should be given as the summation of orbital angular momentum "l" and the spin angular momentum "s" with the symbol J. So according to what is described "j" will be equal to l+s, l+(s-1), …, $|l-s|$. As electrons are moving in an orbit which is in opposite direction to the angular momentum "l" causing a magnetic momentum "μ_l" . Electron spin moment " μ_s" caused by the spin of electron is in the opposite vectoral direction of spin angular momentum "s" . It can be demonstrated as shown in the figure 2.1. below;

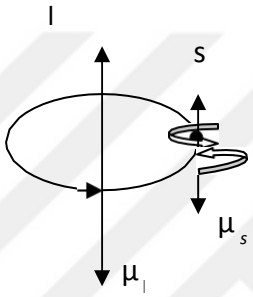

Figure 2.1 Vectoral demonstration of the magnetic moment and angular quantum number

It is described as l – l coupling, the coupling of two orbital momenta. It is said non equivalent when valance electrons are located in different n and/or l energy levels. The total angular momentum is shown with "L" and further orbital momentum couplings will be equal to l_1+l_2, l_1+l_2-1, … $|l_1- l_2|$, and L = 0,1,2,3,… . Likewise total orbital angular momentum quantization requires (2L+1) total magnetic quantum numbers M_s = S, S-1 ,…, -S. Coupling due to spin –orbit interactions which is called L – S coupling gives the total angular momentum J and will equal to L+S , L+S-1, …, $|L-S|$. If we consider an example of two valance electrons in the s^1p^1 , where S will equal to 1 and L will be also equal to 1 so it will have ^1P and ^3P terms where 1 and 3 represents the 2S+1 electron spin multiplicity, since J is equal to 1 and 2 , it will have two terms as $^3P_1$ and $^3P_2$. Electrons that are occupying the same energy level cannot have same spin quantum numbers m_s and as well the same spin magnetic quantum number m_l . As to explain with an example when both $(m_l)_1$ & $(m_l)_2$ = -1 than spin quantum numbers must be either $(m_s)_1$ = ½ , $(m_s)_2$ = - ½ or $m_s)_1$ = - ½ , $(m_s)_2$ = ½ .

2.1.2 Spectral Line Transition

Intensity of the spectral lines depends on the transition probability and atomic population. Characteristics of the transition process are identified by the Einstein coefficients, degeneracy, and the number of the particles occupying the energy level. When an atom of a gaseous element under low pressures is subjected to a form of energy, as an example an electric discharge spark, all atoms are investigated that they are emitting electromagnetic radiation. Liquids, solids and some dense gases are emitting EMR at much higher temperatures. If one investigates the emitted light with a help of spectrometer which consists of all band of colors as like in a rainbow, continuous spectrum will be observed which is typical of matter where atoms are packed closely together. When an atom excites it will emit only certain frequencies of EMR. So if one wants to place this discretely on a frequency line than, atomic emission spectrum is produced as shown below figure 2.2.

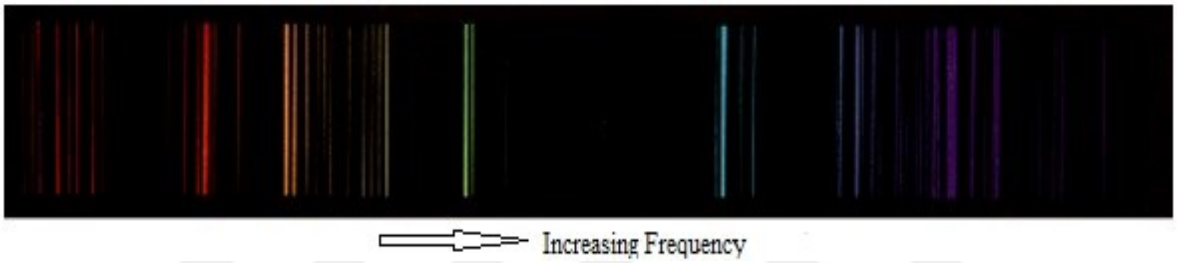

Figure 2.2. Typical Atomic Emission Spectrum

Spectral lines will be formed in series and these series are grouped according to frequency regions (infrared , visible and ultraviolet) of the spectrum. Lines are getting closer with the increasing frequency. It is important to explain the phenomena explained above. At this stage Bohr atomic model is the best to explain the process. As described in "2.1.1 Atomic Structure" principal quantum level of an atom is given as n=1 which is the closest to the nucleus of the atom and said to be in ground state. An atom can always have one ground state, when an electron occupies the higher energy levels rather than the ground state that is said to be excited. An atom can have many excited states. For an example if an hydrogen atom in gaseous state and in the ground state will be excited to an higher energy state, the electron prompted to higher state will not stay as exited and fall down to ground state and this electron transition will result in a photon release of energy given by $E= h\gamma$. This energy is equal to the energy difference of the levels that are involved in the transition. Transitions from higher energy levels to the lower levels categorized and named according to the lower level electron is falling to. Meaning that if the transition is

to the principal quantum level n = 1 than the series of lines are observed in Ultraviolet region of electromagnetic region and called the Lyman Series, likewise the transition from all higher levels to n = 2 quantum level than lines will be observed at visible region of electromagnetic radiation called Ballmer Series. If the final level will be n = 3 than the spectrum will be observed in infrared region of spectrum which is called Paschen Series. This is demonstrated in figure 2.3.

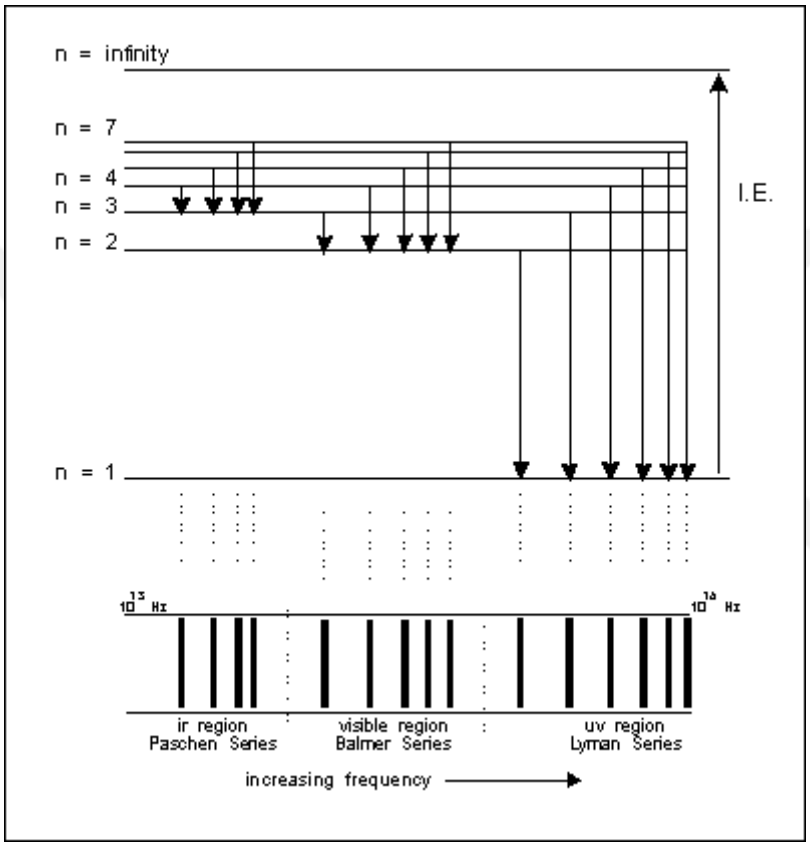

Figure 2.3 Spectral line categorization according to frequency (wavelength)

2.1.3. Spectral Line Broadening

Excitation conditions, transition oscillator strength and degeneracy of electronic states determines the spectral line intensities. Surrounding of the atoms that are excited has an effect on the radiation emission. Optically thin media will not let the re absorption of the radiation in natural emission. Emissions of the excited levels to the ground level, which are named resonance lines can be affected by re absorption occurring at high concentrations. So the line peaks will be broadened and the intensity will be decreased.

2.1.4. Natural Line Broadening

Electrons in the excited energy levels decays until an equilibrium provided. This rate change is given with the equation below ;

$$dN_n / dt = A_{nm}N_n$$

Where N_n is the population in the excited level n, A_{nm} is the Einstein emission coefficient. So the time, that the number of electrons in the n level to drop down to 1/e of its initial value will be defined as lifetime "τ" . Heisenberg uncertainty principle is stating that released energy and time τ can be measured at the same time and the result of those must be bigger or equal to the "h" Planck constant.

Electric dipole moment components has three dimensional components with x,y and z and it should be calculated as;

$$\mu_{x,y,z} = \sum_i q_i (x_i)_{x,y,z}$$

So the transition probability $|R^{nm}|^2$ will be as follows:

$$R^{n,m}_{x,y,z} = \int \varphi_n \, \mu_{x,y,z} \, \varphi_m \, d_x, d_y, d_z$$

$$|R^{n,m}|^2 = (R^{n,m}_x)^2 + (R^{n,m}_y)^2 + (R^{n,m}_z)^2$$

Where n is showing the excited state and the m is the ground state, φ_n and φ_m are the excited and ground level wave functions accordingly.

According to that Einstein emission coefficient can be given as below;

$$A_{n,m} = (64 \pi^4 \nu^3 / (4\pi\varepsilon_0)3hc^3)) \, |R^{n,m}|^2$$

And by placing the Heisenberg uncertainty relation to the above equation;

$$\Delta\nu \geq (32\pi^3 \nu^3) / (4\pi\varepsilon_0)3hc^3)) \, |R^{n,m}|^2$$

Broadening of such type will be lorentzian shape.

2.1.5. Doppler Broadening

Radiation emitted from moving atoms is detected by a stationary detector, which results with a Doppler Effect of shifting. This Doppler Effect creates broadening on the spectral line. Broadening observed from this phenomena is defined by the below equation:

$$\Delta\nu = (\nu/c) \, (2kT\ln 2/m)^{1/2}$$

Here, “c” for the speed of light and the “m” for the mass of the atom. Broadening of this type is much greater than the natural line broadening and in Gaussian shape. This broadening is used to figure out the electron temperature of the investigated atoms and ions by measuring the width of the lines.

2.1.6 Pressure Broadening

This type of broadening observed mostly in gaseous phase, the direct collisions of the atoms are resulting in the broadening in energy of atoms. Broadening of this type is depended on mean collision time “τ” and can be explained by Heisenberg uncertainty principle which is stating that energy and time cannot be identified at the same time.

$$\Delta\nu = 1/2\pi\tau$$

This type of Broadening is in Lorentzian shape as like in natural line broadening

2.1.7 Stark Broadening

Stark broadening observed in the plasma conditions. Moving ions and electrons are creating an electric field in the plasma environment, and so the attraction between particles in the plasma is called stark effect. This created electrical field will apply Coulomb force (F) on atoms. Acting coulombs force on the atom results with the splitting in the energy levels and thus creating a shifted spectral line. $\Delta\nu$ created by shifting and splitting is proportional with the square of the Coulomb force acting on the atoms. Bigger shifts may occur with quadratic Stark effects which are resulting with asymmetric broadening. Studies on this is showing that broadening of spectral lines can be on several sources. [11], [12]

2.2 Laser Induced Breakdown Spectroscopy

Plasma on a target can be produced with a laser having high power is focused on it due to several processes. Intensity of the laser and the conditions in the target media and physical phase of the target is directly relational with the emission radiation from the created plasma. As said before it is obvious that solid, liquid and gaseous materials will have different radiation emission characteristics. It is really complex to analyze the structure of the plasma, so several studies have been done on this subject. [13], [14]

I will be mostly focusing on the plasma created on solid species as the study based on species of solid thin films. Intensity of the spectral line of the species investigated will give so much data as well the quantity of the atom analyzed with utilization of the calibration curves of the same element prepared under similar conditions. Here in this study I just

worked for detection of the investigated element rather than its concentration in the sample in order to develop a structural analyses method.

Created plasma depends on the size of the laser focal spot, the pressure of the media, composition of the target, laser characteristics like wavelength and intensity of the laser beam. The hot plasma is created on the edge of the target and passes through several modes as expansion wave created which is called absorption zone. Created plasma pushes the surrounding media forming a shock wave. Laser absorption results in Bremsstrahlung radiation due to free electron transitions. The first emission is the blackbody radiation and is decaying much faster than the specific line radiations. After the plasma cools down characteristic spectral lines can be observed. Ionized and neutral atoms start to be observed approximately 500 ns after the plasma initiation.

2.2.1 What is LIBS

The analytical atomic spectroscopy is developed with a relatively high speed within last four decades because of the invention of high power lasers and the development of the array detector. Having these inventions and developments led the invention of laser induced breakdown spectroscopy (LIBS) which is also named as laser induced plasma spectroscopy (LIPS) and laser spark spectroscopy (LSS). In some sources also it may be named as laser optical emission spectroscopy (LOES).

Commonly in LIBS applications a low-energy (tens to hundreds of mill joules) laser is used in pulsed mode to generate a micro plasma which is vaporizing a very small amount of the investigated sample. With the plasma production it is obvious to have spectrum from the excited atoms in the investigated sample, this spectra is than used to have qualitative and as well quantitative information about the species (atoms) in the sample. Targeted samples may be gases, liquids, aerosols and mostly the solids. LIBS applications are in very wide range from sampling iron and steel, contamination detection in soil, the metals which are used in nuclear reactors for the degradation, age determination of artworks, bones of mummies and other skeletons for evidence of the probability of water contamination in the past decades, and detection of aerosols which are emitting from smokestacks of some industrial processes or during some machine operations. Especially in last 5 years very new applications have been developed worldwide, like sampling biological materials, explorations based on planets and security development for homeland. There are some many improved techniques developed and causing the LIBS

instrumentation available commercially. Different experiments are deriving more improved computational and theoretical plasma formation and expansion models.

The interest of this analytical analyses method is mostly because it is capability of multi elemental results, very low quantity of sample need, detection capability of nearly all elements, fast measurements and resulting and no sample preparation process. The major issue and the difficulty of LIBS method is calibration hardness, which is the most attractive topic of the current studies and research activities.

The most commonly used LIBS system is schematically given in the figure 2.4. The technique is working with a low-energy and pulsed laser (tens to hundreds of mJ per pulse) and a lens to focus and form plasma on the target which vaporizes a small amount of the targeted sample. Spectrum light from the plasma light is collected. With the help of a spectrometer, EMR emitted by excited atoms and ionic species present in the plasma is separated by a spectrometer and a detector records the light spectrum and converts it in to signals and by the help of a computer and small electronics the signals are converted to digitized data in order to display the results on a screen.

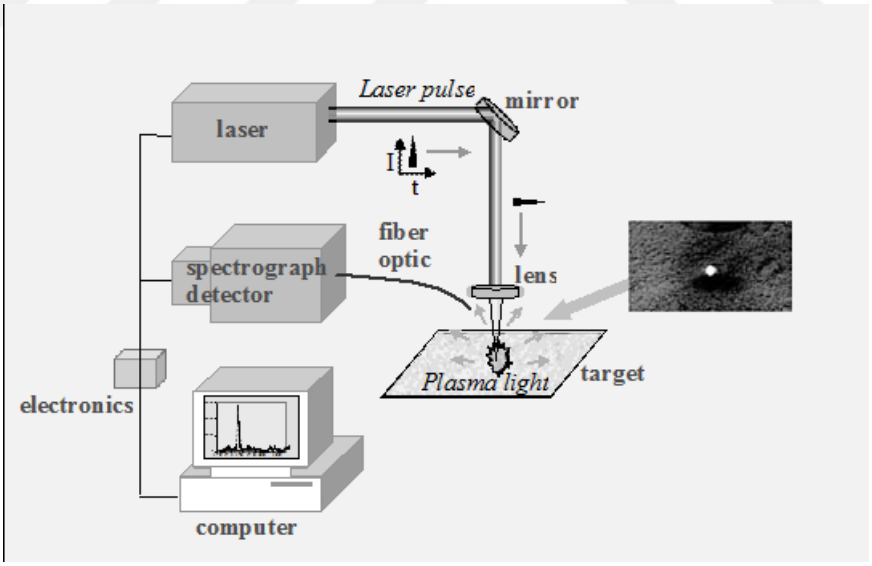

Figure 2.4 Simple schematic for the Laser Induced Breakdown Spectroscopy

Figure 2.5 is showing the photograph taken as the laser pulse generates a spark (plasma of the atoms of the sample targeted) which is emitting EMR according to the specific wavelengths of the atoms in the target sample.

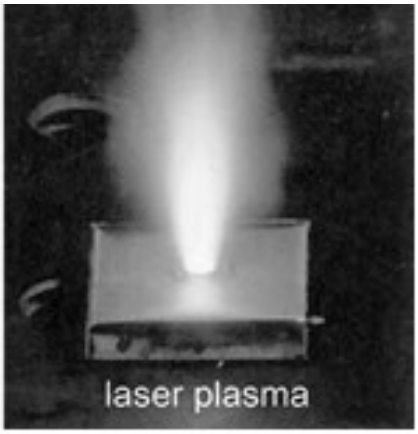

Figure 2.5 A spark generated by laser shot on a sample

2.2.3 How LIBS Spectra Created

LIBS is a charming technique compared with the other spectrometric type of elemental analyses, as it is easy to focus the laser beam with a simple optic focusing on the sample need to be analyzed. Micro plasma of sample created could be in all kind of phases like solid, gas, liquid, and aerosols. However the physical and chemical phenomena lying behind, like initiation of the plasma and then formation and decaying of it are very complex processes. First of all absorption of the energy transferred to the sample by the radiation is collision of photons, electron, and atoms or molecules. For example the laser pulse creates a shockwave in liquid and gases by which energy will be transferred with the conduction, radiation and the shockwave. When the sample is projected in a vacuum condition, formed plasma will expand and escape freely with different speeds than in atmospheric conditions. Specific energy level excitations in different atoms are differing from each other and complex. These excitations depend on interactions with atoms and molecules combined under matrix effect category and thermodynamic equilibrium. After the laser pulse is finished, created plasma starts to decay in typical from 1 to several microseconds, which is directly dependant to the laser energy used. This decay time will be shorter in vacuum conditions. Observed spectra will be changing with the plasma decaying time.

A plasma is defined as combination of atoms, ions and free electrons, which is overall electrically neutral on the other hand charged types acting together. There are different parameters for categorization of plasmas, most important and basic one is the

ionization degree of the plasma. If the free electrons is %10 by ratio to other species in the plasma, it is said that a plasma is weakly ionized. Likely it is said to be highly ionized plasma if the plasma is with so many atoms lost its electrons causing very high ratio of electron to ion.

Plasma formed with LIBS is mostly named as weakly ionized plasmas. In figure 4, the plasma initiated by a single laser pulse is seen. At the first stage of the plasma formation the ionization is respectively high. As soon as electron – ion interactions starts neutral atoms and the molecules are formed. A very fast decaying process takes place starting with the electron – electron interactions coming from bremsstrahlung event which is the acceleration or deceleration of electrons due to collisions. And after when a free electron captured by an atomic or an ionic level with emitting a photon and losing the kinetic energy it had, electron recombination occurs. Investigation of the LIBS plasma by means of time gives us the spectrum of the interested species in the whole plasma. In figure 4 the symbol t_d is representing the time delay starting from the first initiation of the laser pulse to the first detection window opening in the spectrometer, during this time spectrum signal is accepted, t_b is the time that detection of the spectrometer is valid. It may also be possible to work in double-pulse mode which means to two consecutive laser pulses either created by the same laser source or two different sources optically targeted to the same point [15]

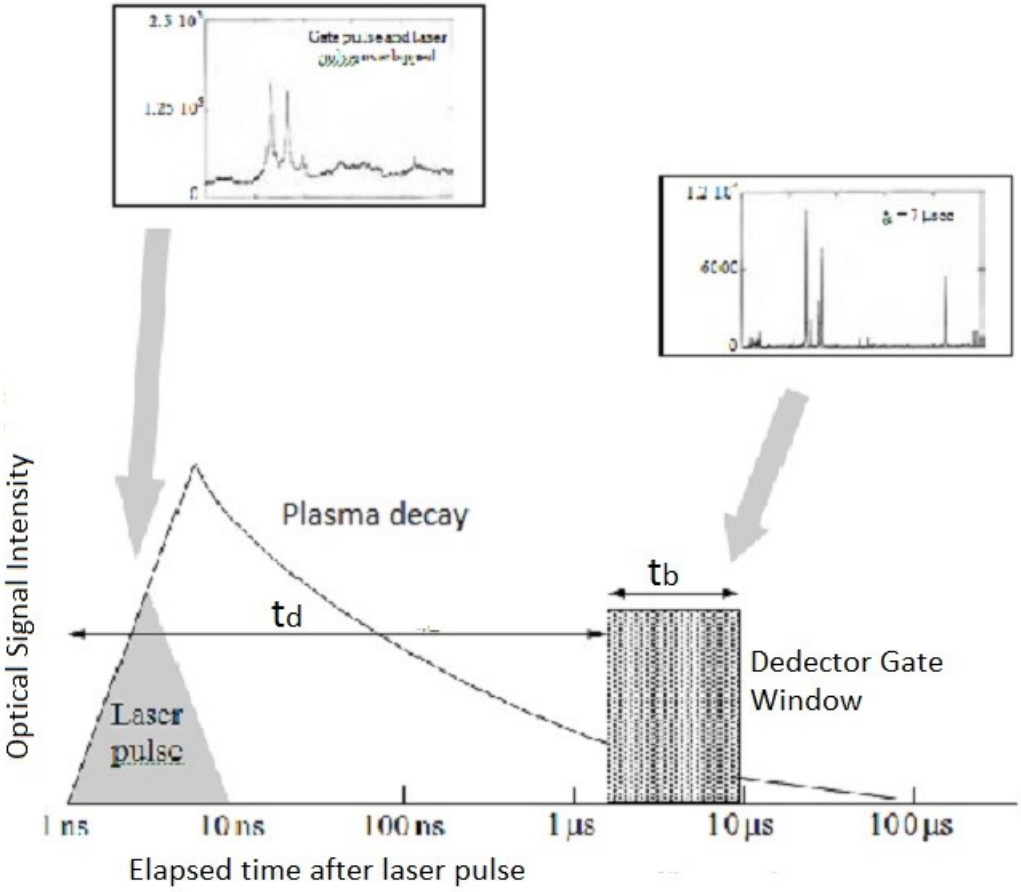

Figure 2.6 Schematic view of the plasma created by a single laser shot. Illustrated spectra can be seen on the figure for different timings

Above figure 2.6 is showing a plasma created in 1 atm air with a laser pulse of Nd:YAG laser with 5 to 10 ns and 1064 nm. For lasers with longer pulse withes like a pulse created with a CO_2 laser, the pulse decay time will be increased in that range and likewise if the laser with short pulse withes should be used (e.g. pico – femtosecond lasers) the pulse decay time will be shorter. Pressure of the media surrounding the plasma has also significant effect on the plasma lifetime, such that if the ambient pressure decreases or increases, plasma life time will decrease or increase accordingly as there will be less obstruction acting on the plasma, which means weaker trapping and recycling of energies in the plasma volume. In LIBS low energy levels are used to form plasma, which are typically 5% - 10% ionized at the very first initiation period.

2.3 Components Description of LIBS

LIBS is an atomic emission spectroscopy which is based on plasma so it also have similar instrumentation like other atomic emission spectroscopy methods. The strong side of the LIBS is the relatively high energy laser it uses than other type of spectroscopy

methods, this high energy is used first to prepare the sample needed and then excite the atoms to emit light in the sample to be investigated. Laser beam which is focused on the target first ablates a little amount from sample which means preparing the sample. And in a couple of nanoseconds after the ablation of a small portion, a micro plasma formation takes place in which the concerned atoms are excited. Plasma formed just above the target continues the excitation even in the absence of laser beam. Small ablated portion vaporized from the plasma so as a result the atoms are excited.

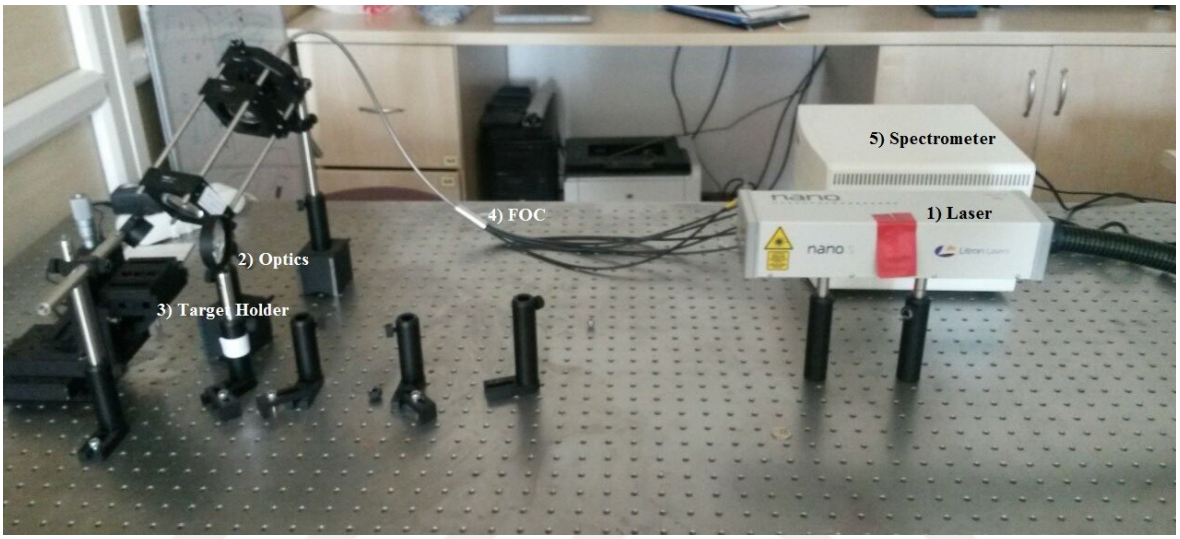

Figure 2.7 The LIBS apparatus used in this study

The main components of the system shown in figure 2.7 listed down as:

(1) Pulsed laser which is generating optical high energy pulses which is used for the initiation of the plasma on the target.

(2) Optical system that is consists of mirror and lenses used to target the laser light on targeted sample.

(3) Target holder, to stabilize the samples and to move them gradually with a compass

(4) Another optical light collection system (lens, FOC) to direct the emitted light from the samples to the system of detection.

(5) Detection unit which is used for spectral filtering and dispersing the emitted light

(6) Computerized electronics for laser firing timing, gating the detector for specific time window and storing the spectral information received.

2.3.1 Laser Fundamentals

Laser basic operation and the structure and working principles of some specific lasers are described in numerous sources by detail[16]. In this study the definition of the laser will be limited with the description and structure and working principle of the flash lamp - pumped Nd:YAG laser that is commonly used in LIBS studies and applications in the literature. A very draft and basic schematic of a Nd:YAG laser is given in Figure 2.8. To explain briefly, a flash lamp is used to produce a wideband light, that is also called as pumping light and which is containing all regions of EMR (i.e. UV, IR and Visible). Little portion of this wide band EMR generated by flash pump is captured by the ions doped in the special material called "lasing" of the laser; in our example it is Nd ions which are doped in YAG crystal (YAG:Yttrium Aluminum Garnet). A strong flashlamp used to generate a phenomenon called stimulated emission. This is produced by the photons coming form flashlamp with the same frequency of lasing materials atomic transition frequency from upper level to the termination level. When these photons enters to the lasing rod, starts travelling through the rod and causing an amplification of lasing transitions in the lasing material which called population inversion. Also to have significant increase in explained amplification of the generated light by this process, lasing rod could be covered with two mirrors and causing extra amplification by reflected light with the same wavelength of lasing transition wavelength.

In LIBS applications, laser pulse energies are mostly in the range of 5 MW which is needed to create the plasma on the focused target sample. In order to create this high powers a pulsed and Q – switched lasers are used. In Q – switched lasers, a shutter is used for photons that have the same wavelength of laser wavelength to prevent these photons from travelling whole rod path instead letting them out from the rod with high powered but short pulsed beams by a semitransparent mirror called output coupler. Pulse durations for such beams are in magnitude of 5 ns to 10 ns for most of the Nd:YAG lasers. This pulses are so short because population inversion process depletes so quickly with lasing termination very quickly after lasing begins.

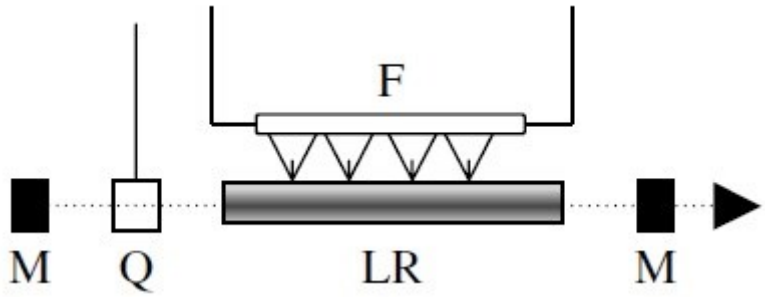

Figure 2.8 Schematic for (Nd:YAG) F: flash Lamp; LR: Lasing Rod; M: Mirror; Q: Q – Switch

2.3.2 Laser Types

In LIBS applications Nd:YAG lasers mostly utilized but of course also there are other kind of lasers used accordingly with the wavelength and application requirements, in Table 1 some other type of lasers are listed, these listed lasers are also can be used in different requirements of LIBS applications.

Table 1 Common Types Of Lasers

Type	Wavelength(nm)	Pulse with(ns)	Rep. Rate(Hz)	Comments
Nd:YAG (solid state)	1,064,532,355,266	6 – 16	Single Shot to 20	Wavelength easily changed by using harmonics Co mpact and easy to install High beam quality
Excimer (gas)	XeCl : 308 KrF : 248 ArF: 194	20	Single Shot to 200	Dual-pulse capability Beam quality not good as Nd:YAG Wavelength in UV scale
CO_2 (gas)	10600	200	Single shot to 200	Gas or gas flow should be changed periodically Beam quality not good as Nd: YAG
Microchip	1600	< 1	1 – 10 K	Better beam Quality Rep rate is high Stability in shot by shot

Nd:YAG lasers are commonly preferred in variety of applications [17]. As because they are reliable, compact and easy to use sources of laser pulses with high focused power density. Also intrinsic wavelength of these laser can be easily shifted to form wavelengths of UV region to IR region of the radiation.

Irradiance of the Laser pulse means the intensity of the light to generate laser plasma, and this is given by W/cm^2 as unit of irradiance or sometimes it can also given as photons / cm^2. Energy of the laser pulses in LIBS applications are mostly from 5 mJ to 500 mJ in magnitude, which also means that $5x10^6$ photons to $5x10^8$ photons (photon energy ~

10-19 J). Also it should be kept in mind that these photons will be present in a short light pulse with approximately 10 ns duration.

Monochromaticity of the laser beam means that light beam is not broadband and do not include the different ranges of wavelengths. Laser beam is special for having very narrow wavelength range which is produced with well-arranged transition in the lasing media. As mentioned above the laser bandwidth is typically < 0.001 nm. Actually according to excitation properties the monochromaticity is not so crucial, laser can be produced nearly in all regions of spectra (IR, visible and UV). Some specific wavelengths interact more strongly with some materials so that the wavelength is becoming important for ablation. High monochromatic laser beam is not always an important feature as because bulk materials absorption spectra are mostly slowing varying functions of wavelength. In some LIBS applications, monochromaticity may be important, so that some optical filtration devices may be used to get rid of this feature and in some applications reflecting the narrow band and passing the broad band of the laser light could be a case.

Directionality is another feature of the laser beam and means the ability of the beam to travel long distances without enlarging the beam radius and remain as collimated. This property is important for LIBS plasma creation as it gives the ability of stand – off and remote. Stand – off is the ability of projecting the laser beam over the target as collimated beam in open atmosphere over meters. Remote means how easy of a laser beam to carry with a FOC. Both features needs good directional beam quality laser. A laser that is operating at Gaussian mode which is called as single lowest order mode, produces a laser pulse which is replicating closely a uniform flat wave that is having fixed phase distribution across wave front. Such type of pulse coming out of the coupler of the laser with diameter d will be extremely directional. The distance for such a parallel beam is given with the equation; $\nu d^2 / h$ and called Rayleigh range. After the distance given with the equation, the angular spreading of the beam is given as A8 and is described with d/h which is called beam divergence.

2.3.3 Optics Used in LIBS

Laser shot produced by a laser system described in "2.3.1 Laser Fundamentals and 2.3.2 Laser Types" above must be focused on the sample by a lens and mirror array as shown in Figure 2.8. As a common practice, a single lens is utilized for focusing laser beam to a tiny spot on the target to produce analytically useful micro plasma which is

shown in figure 2.8 a). In some complicated systems which are requiring an adjustable focusing needs, for example in an industrial analyzing process with a requirement for adjusting the distance of lens to sample because of case to case variations of distances between samples and monitoring unit. For such cases multi-lens system may be needed to be used with the relative positions of the lenses which are adjusted in order to focus the beam on the target as shown in figure 2.8 b). It is also possible to locate the focus on the target by using a mirror as in figure 2.8 c).

According to the system requirements, for the collection of the plasma light and for directing it to the detection system which is a spectrograph and a detector in most of the cases, a lens system or a mirror system can be used. Of course the single lens system is the easiest way of optically arranging the plasma light to be focused on the detection system, on the other hand systems using more than one lens may be required in some specific cases of applications. Unless it is not build up specifically to avoid the effect, lens systems have the disadvantage of showing chromatic aberration [18], in such situations focal distance of these systems will be depending on wavelength as seen in Figure 2.8 d). This issue is because of the fact that refractive index of optical materials are depend on wavelength. As an example refractive index of quartz crystal is decreasing with increasing wavelength, so this will end up with an increase in the focal length and also the opposite of this phenomena is valid in opposite change. So the most important advantage of the mirror systems can be understood with this wavelength dependency of the lenses. In mirror systems wavelength can be focused easily to same distance without changing. But also mirror systems has a disadvantage, such that astigmatism and coma observed when a spherical mirror in an off-axis configuration is used [20] and this will distort the resulting image on the target.

In common LIBS applications, spherical lens is used for focusing the laser beam on the target, which is radially symmetric for a Nd:YAG laser. This makes the beam on the target a circular spot and produces the plasma.

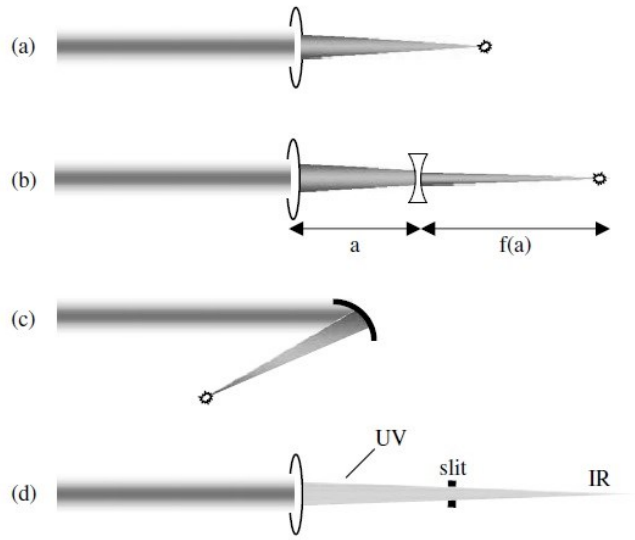

Figure 2.8 Focusing variations to observe laser induced plasma

2.3.3.1 Fiber Optics For Light Collection

Fiber optic cables (FOCs) are a must to use with LIBS because they are the most simple and easy way of collecting the plasma light figure 2.9. FOCs are used as it is not practical to place the detection system close to the target. Before the invention and utilization of FOCs, laser beam was directed to the entrance slit of the spectrometers without any other device in between or the intensity of the laser plasma was sufficiently high that it would be enough to receive sufficient amount of light with the spectrometer. It will have great effect on the information received from the spectrum even if a little change in the position of the plasma, this is happening because emissions intensities and relative intensity are depending to the plasma position so much.

Figure 2.9 Fiber Optic Cable (FOC)

A typical FOC produced by fused silica is shown in figure 2.10 as schematically. Numerical aperture means the total internal reflection of the radiation entering the FOC with its acceptance cone. If the entering light is directed to the fiber within its numerical aperture which is ~ 26^0 for fused silica, all reflections will be with high efficiency. Although the plasma emits the light in UV region, UV light induced phenomenon is not an issue which is degrading the transmission efficiency of the FOC used in the design of the system

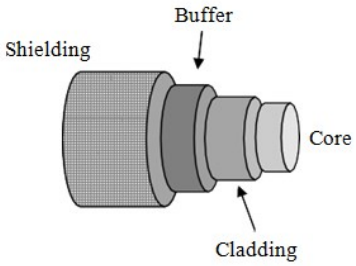

Figure 2.10 FOC Structure

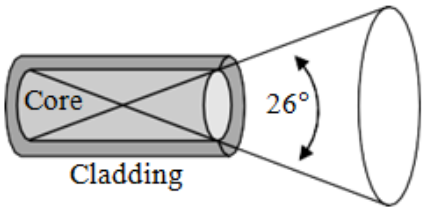

Figure 2.11 Acceptance cone of a Fused Silica FOC

Fiber cables core diameters are generally varying between 50 μm to 1 mm. The fused silica, which is a common material for FOC, used can be made as low or high OH containing, depending on the usage requirements in the system. With high OH fibers it is possible design a system to work in UV & Visual range of the spectrum. On the other hand with low OH one can work in near IR region of the spectrum because of the low water

content which is typically < 2 ppm and corresponding to a lower absorption of the light. Cladding material is used to improve the the guiding property of the fiber with a lower refractive index $n_c < n_f$ than the refractive index of the core fiber. Mostly fluorine doped silica is used as cladding material which is generating 0.22 numerical aperture, given as NA. Where NA = $(n_f^2 - n_c^2)^{1/2}$. There is another coverage material over the cladding material which is called as buffer material used for reinforcing the core and to prevent the scratches and other physical damages that may defect the cladding material. Composition of the buffer material is depends on the environmental requirements that the fiber is going to work. For example a polyamide buffer can supply a working temperature range of -100^{0}C to 400^{0}C, while for higher temperatures of working conditions a gold buffer will be a solution which gives a protection range of – 90^{0}C to 750^{0}C. There will an outmost shielding which is mostly based on reinforced PVC or shielding with metal.

With help of FOC, either laser plasma emission can be carried to the spectrometer or the laser pulse can be transferred to the optic system which will than focus the pulse on the target, which will reduce the alignment problems of the laser beam.

FOCs can be produced in different lengths according to need of requirements and with different standard of connection types. Also the cable can be modified according to the spectral needs for the spectrometer system, for example UV and Visible (200 nm – 800 nm) region, IR and Visible (350 nm– 2000 nm) region or UV (solarization resistant below 230 nm).

2.3.3.2 Spectrometers

A spectrometer is an instrument that spatially separates the colors of light into a frequency (wavelength) spectrum. The spectrometers consist of a diffraction grating (or prism), an entrance slit, and collimating mirrors or lenses. Diffraction gratings in spectrometers separate incoming light by wavelength. Diffraction grating consists of many grooves typically (10^5) that reflect collimated parallel light. The angles and widths of grooves on glass plates depends upon the designed spectral resolution and wavelength region of interest figure 2.12. Light that is reflected from the grooves generates destructive or constructive interference. Grooves can be defined as light sources since they reflect incoming light with a width of d which is approximately equal to the average wavelength λ of the spectra. Difference between the paths of light reflected from two adjacent grooves

produce constructive interference. The grating equation is as follows:

$$d \sin\alpha \pm d \sin\beta = m\lambda$$

In the above equation α is giving the angle, normal light to incident light, β is giving the angle, normal light to reflected light.

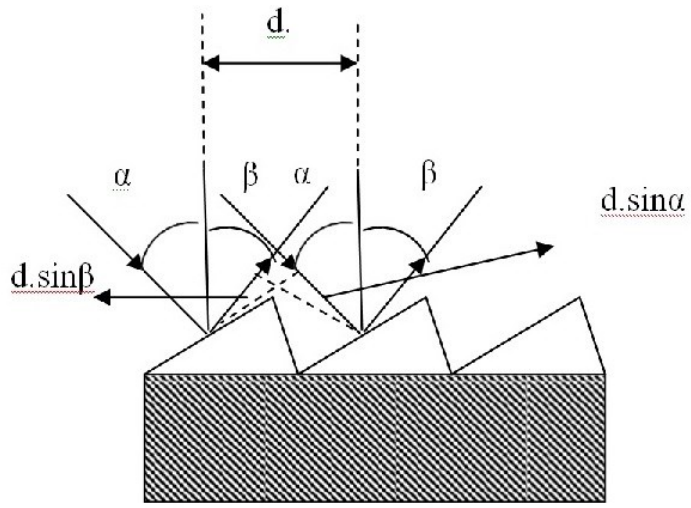

Figure 2.12 Incident light reflection in a groove

Reflection from grooves needs to be adjusted depending on the type of spectrometer. The blaze angle between the groove normal and the incident light is determined according to the desired spectral range and spectrometer type. The angular dispersion can be defined as $(d\theta / d\lambda) = n / d\cos\theta$. The resolving power of grating is given by $R = nN$, where N is the number of grooves. Depending on the design, there are some different spectrometers, Czerny-Turner spectrometers are widely used in spectrometric applications. The grating, entrance and exit optics are inside the spectrometer figure 2.13. Gratings typically have 100 to 4800 grooves. The spectral resolving power is the wavelength divided by the difference between two consecutive wavelengths. Diffraction limit line profiles are achieved if the central maximum coincides with the adjacent wave minimum. Although spectrometers have the same structure as monochromators, they can detect different spectral ranges and large region simultaneously and successively. The signal which is received by the detector depends on the area of the exit slit and the spectral intensity.

Charge coupled device (CCD) arrays with Czerny-Turner spectrometers can detect with low integration times whereas although photoelectric recording is more sensitive it requires longer detection times.

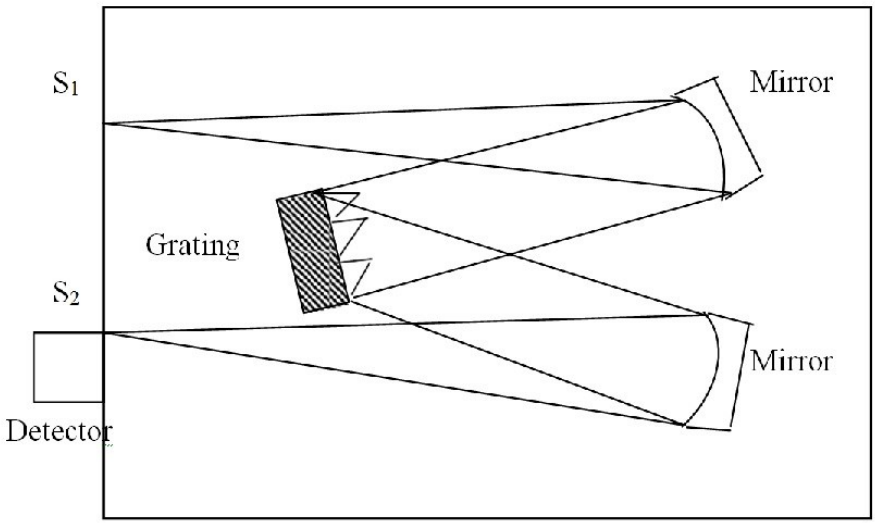

Figure 2.13 Czerny-Turner spectrometer schematic drawing

A Paschen-Runge spectrometer consists of several monochromators. A Rowland circle with grating and several slits attached is the main structure of this spectrometer. The grating is fixed and does not move figure 2.14. Spectral wavelength coverage (UV to NIR) needs too many photomultipliers to detect the signal. In the original Paschen- Runge spectrometers, photographic plates were used for detection, enabling recording the entire spectrum.

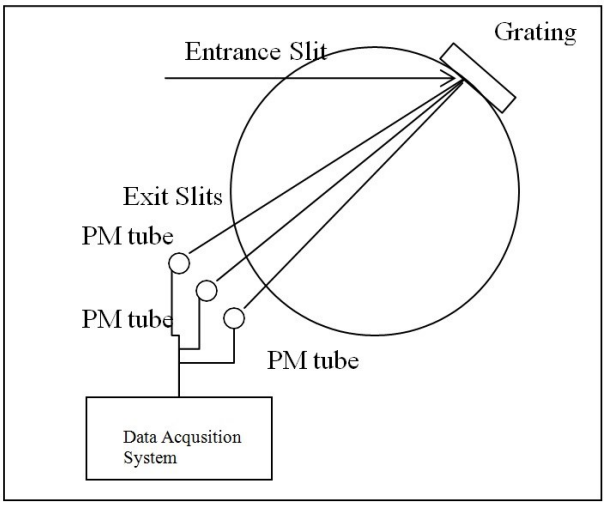

Figure 2.14 A Paschen spectrometer schematic drawing

An echelle spectrometer is made up of high dispersion echelle grating, lenses and mirror. In this kind of spectrometer grooves are far located than each other. As it is mentioned, the power of resolving is dependent on the number of grooves and the spectral order. Resolution of the echelle spectrometer can be improved by increasing the blaze angle and the spectral order, but the overlapping issue is unavoidable in these kind of spectrometers. A prism can be located perpendicular to the other gratings and can be used as second grating unit. So the prism can be used as determining the wavelength coverage before light is dispersed by the echelle grating. ICCD and/or CCD detectors can be attached to echelle spectrometer in order to make the analyses of the spectrum which is well intense and resolved. In common an echelle grating has 0.12 nm/mm average reciprocal linear dispersion and 0.003 nm resolution. This is the one of the biggest difference between echelle spectrometers and the ordinary spectrometer which is the grating density. Such that in ordinary spectrometers grating density is 1200 while in echelle it is 79. Although an echelle grating can cover wider spectra and region, high limit of detection can be measured in some application corresponding to Czerny – Turner spectrometers. But this does not mean that it has less detect ability. There are so many usage and application with echelle spectrometers with ICCD detectors which are giving reasonable results compared to other types of spectrometers.

2.3.3.3 Detectors

A photo detector is a photon sensor that is commonly located on the exit slit of spectrometer and used to record the spectra maintained. Photo multipliers tubes (PMT) and the solid state detectors are commonly used detectors with the spectrometers for all types of spectroscopy. The detection of the signals is time dependant and needs to be time resolve detection to those systems are correlated with adjustable time delays and signal integration times. Detectors with high quantum efficiency and fast temporal response are chosen to connect with the spectrometer application.

Photo multiplier tubes are very sensitive light detectors, which is creating a current proportional to the intensity of the light that is absorbed. Tubes are having photo cathode dynodes with a gain of 10^6 to 10^7 scale for incident photon. It has spectral bandwidth of 6 to 100 nm with a single channel as shown in figure 12, Noise of the PMT is coming from the fluctuations in the incoming signal, fluctuations in the amplification process and the dark current of the system. The created current is related with the applied voltage to the

detector and converted to a signal by an analog to digital converter. Noise which is coming from the dark current of the detector is the main issue for gated detection purposes. This noise can be avoided by cooling the detector and by using a boxcar averager – gated detection.

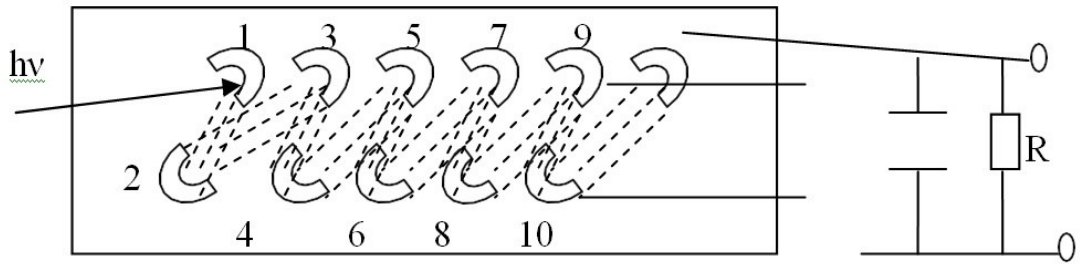

Figure 2.15 Photomultiplier schematic drawing

Photodiode array (PDA), charge coupled device (CCD), charge transfer device (CTD), and coupled injection device (CID) devices are also solid-state detectors. These devices transfer photons to charge by pixels or semiconductor elements.2 PDAs consist of several diodes integrated within a chip, forming a photodiode array. They have up to 2048 diodes in one dimension. Applying potential difference V to the p-n diodes and illuminated with light, the photocurrent generated discharges the diode capacitance figue 2.16 a) Metal oxide semiconductors (MOS) switch that is connected to the photodiodes recharges the photodiodes. High temperature has a major effect on the integration time, increasing the dark current and reducing the signal-to-noise ratio. For most of spectroscopic applications such as plasma diagnostics and induced incandescence, gated detection is essential to analyze very weak signals, especially in high background. CCD and PDA detectors coupled with Echelle spectrometers provide signal integration times in the nanosecond to microsecond range.

Quantum efficiency is the ratio of rate of photoelectrons divided by rate of incident photons. CCDs which have replaced PDAs have the ability to change charge capacitance of MOS capacitors, providing 90% high quantum efficiency figure 2.16 b) CCDs are mostly preferred because they have low dark current with respect to other detectors (PMTs, PDAs) [19]. They can be used for in 350-900 nm spectral range. Being small and compact and also very easy to couple with a spectrometer in most of the case an ICCD or a CCD detector is preferred to be use with the spectrometry studying requirements.

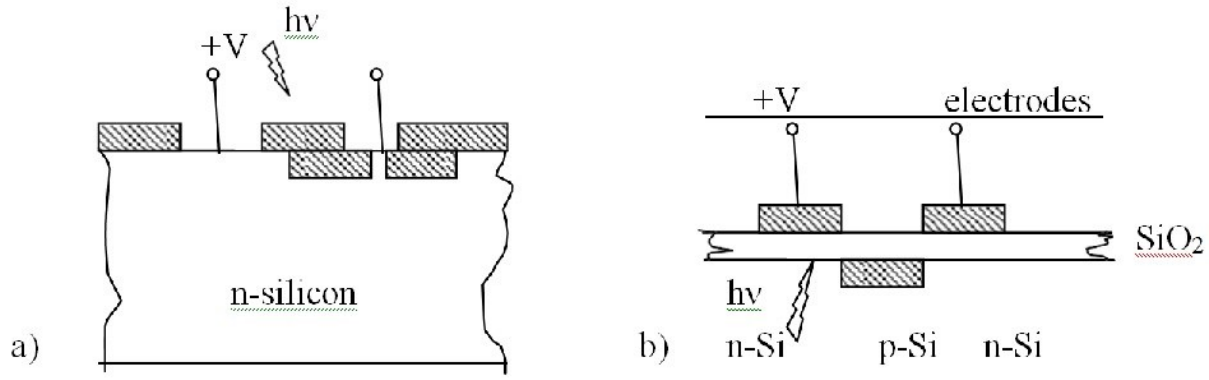

Figure 2.16. a) Single diode array b) CCD array

CCDs catch electrons that are generated from electrons and holes by detecting incoming light. Analog-to-digital converters in CCDs help to transform the signal from where it is created by the electrons in to the final form. ICCDs have image intensifier that work as shutters opening and closing in nanosecond time scale. As has been mentioned for PMTs, the photocathode in ICCD changes photons that the absorbed into images by producing electrons by the photoelectric effect. Material of cathode, photo emissive material thickness and the wavelength of incident radiation is highly affect the photocathode's quantum efficiency. A micro channel plate (MCP) consists of a glass with a micro channel structure system figure 2.17. Electrons are transformed to photons and amplified, and focused on the phosphor screen of the micro channel plate (MCP). The MCP gate voltage is generally in 200V which is sufficient to accelerate electrons up to high voltages. The photocathode has the most important role for detection because it creates electrons independent of the incident photons, and determines the quality of the ICCD. Gating capability depends on the voltage that is applied to the photocathode which determines the shutter switching for the shortest gate delay times. Gate delay times can be changed mostly from 1 to 3ns with using conductive nickel. For time resolved measurement such as LIBS and LII, the detector should have gating capability.

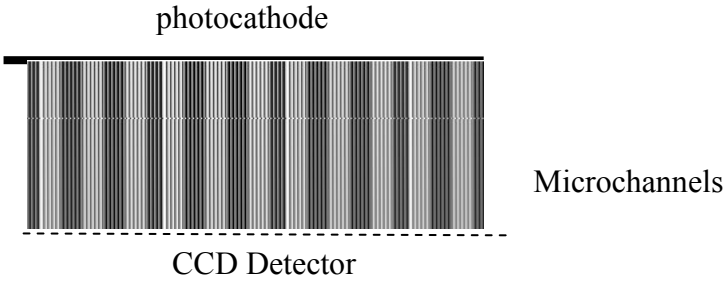

Figure 1.7 Schematic drawing of a MCP detector

2.4 Importance of ZnO: Ge nanocomposite thin films

In the study to find different solution for high efficiency solar cells, intermediate band gap cells have become very popular. The reason that they have been studied so much is the energy level of a confined state in a quantum dot in essence is acting as an intermediate band. So semiconducting nanoparticles embedded in a semiconducting material with a wide band gap is expected to form an intermediate band which makes the transitions from valance to intermediate band and intermediate to conducting band possible thereby causing enhanced spectral response.

Most of the studies are done by Si and Ge nanoparticle embedded in wide bandgap semiconducting oxide matrices. Indirect bandgap produced with Si and Ge atoms creating an electron-hole pairs with a long life time when corresponded with the direct band gap materials. Based on the theoretical studies, Ge is predicted to show a significant quantum confinement effect below 24nm Bohr radius. This limit is much above that of Si which is approximately 5 nm Bohr radius. [20], [21]

Ge has and energy difference of 0.12 eV between direct and indirect band transitions. This specific condition makes it attractive for electronic structure change near band edge. Studies show that Ge nanoparticle embedded oxide materials have significantly changed optical behaviors which is caused by the quantum confinement of electron hole pairs in Ge nanoparticles. [22], [23] The structure of Ge nanoparticles and the nature of the interface between oxide material matrix must be understood to interpret this behavior change.

In most of the studies, SiO is used as the oxide material, however ZnO with a larger exciton binding energy (~60 meV) compared with GaN and ZnSe which are also wide band gap oxides, seems more appropriate as embedding medium. Also ZnO has high resistance to photo corrosion. Ge and ZnO electron affinities are also close enough to each other which is causing the charge carriers generated by light are not affected by confining potentials. Also, valance bands of Ge and ZnO in heterojunctions have high energy difference resulting in very low leakage current.

In the literature there are different studies on both Ge and Si nanoparticle embedding methods. There are different methods for preparation of Ge nanocrystal embedded ZnO thin films in current literature. T. Zheng et al. used the sputtering of Ge and Zn ions in vacuum condition and used the sample annealing method at 580^0C for 60

minutes [24]. A. Ceylan et al. used the similar way of sputtering Ge and Zn ions, but tried the Rapid Thermal Annealing (RTA) instead of conventional method for observing the local atomic properties and as well the structures of the samples [25]. Also in another study results are discussed for sputtering of Zn in presence and absence of O^- ions in the preparation of same structure [9]. We used the same sputtering method for Ge and Zn ions on Si substrate and RTA was performed for 30s, 60s, 90s accordingly except one sample which is left as prepared. Preparation sequences of the samples are given in detail in experimental section of this study.

3. Experimental

3.1 Preparation of ZnO: Ge nanocomposite thin film

In this study, Ge nanopartical embedded ZnO thinfilms are investigated as it has a promising photovoltaic properties as a result of theoretical background described in the previous chapters of this study. So it has a high importance to analyze the homogeneity of the structure formed by means of both depth and layer formation surfaces in order to figure out the structural efficiency dependency for this type of solar cells with further electrical characteristic studies.

Same process is followed, like in most of the studies [22], [26], [27] which is sequential sputtering of Ge and ZnO layers followed by a furnace annealing. Multilayer thin film samples were deposited by using 2 inch Ge and ZnO targets having 99.99 percent purity. A power of 100 W R.F and D.C is used for sputtering respectively on Ge and ZnO targets under 45 mTorr Argon gas as sputtering gas. Before placing the Si(1,1,1) substrates on a rotating substrate holder, the substrates were cleaned in a ultrasonicator using in order of acetone, alcohol and distilled water. Substrate holder was kept at ambient temperature during the sputtering process. 10^{-6} Torr is achieved in the chamber before deposition started and flushed with 500 mTorr Ar gas in order to get rid of any residual gas contents. 5 Ge layers were deposited between 6 ZnO layers by sequential sputtering. By controlling the deposition times, the thicknesses of ZnO and Ge layers were adjusted to be around 90 nm and 20 nm, respectively. Top ZnO layer is deposited for a longer duration to avoid diffusion of Ge atoms during thermal process. In order to form Ge nanoparticles out of Ge layers, rapid thermal annealing (RTA) process were employed. RTA was done at 600^{0} C for 30s, 60s and 90s. More details of sample preparation step can be found elsewhere [25]

3.2 LIBS Experimental Setup

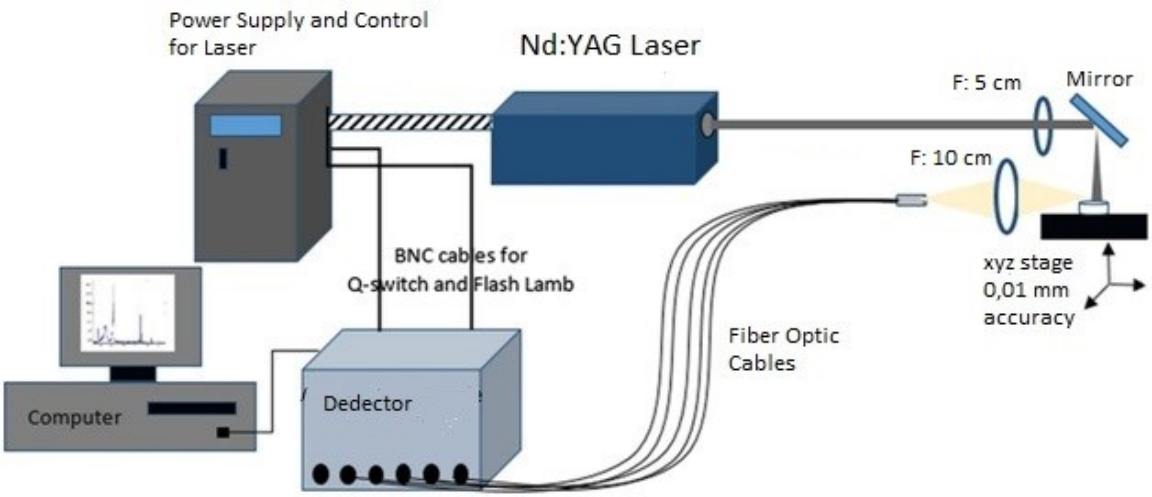

Figure 3.1 Experimental Setup Drawing

Laser shots are obtained by using a Nd:YAG laser with max power 50 mJ and wavelength 1064 nm. LIBS spectra is collected by Aurora 5 channel spectrometer. Laser shots are focused on the sample from a convex lens which have 5 cm focal length 1 inch diameter, spectrum lights are directed to the fiber optics acceptance cone with a convex lens which have 10 cm focal length 2 inches diameter, as shown in Fig 3.1.

3.3 Optimization of the setup

It is really crucial for LIBS to figure out the optimum energy of laser pulse and the delay need to be given after the laser shot to detect spectrums. Sample of a ZnO:Ge thin film is chosen with 3 min sputtered and 90 s annealed at 600^0 C to determine the optimum energy and delay to be used to get the acceptable Ge spectrum with a SNR minimum of 20. Optimization is performed by having consecutive shots from 5 different locations on the sample. SNR for Ge spectrum peaks are calculated for every 2^{nd} shot of each location and plotted on a graph, which I used as method for optimization of LIBS energy and gate delay. Second shots are taken in order to avoid any impurity signals which may overlap the intrinsic Ge signal and should increase the baseline fluctuations on the spectrum and resulting in increase of STD values. 1^{st} shot spectrum with correspondence to 2^{nd} shot is shown in figure 3.2 which is supporting the above theory for 2^{nd} shots.

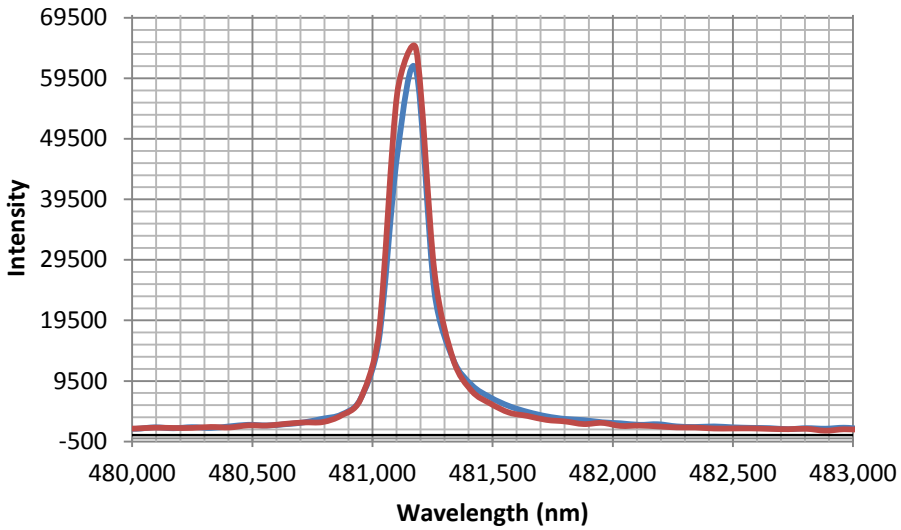

Figure 3.2 Zn Spectrum at 401,103 nm in 1st and 2nd shots (Red line is indicating the spectrum from the second shot)

As it can be seen in below figure 3.3, 19,7 mj pulse energy with 0,7 ms delay is the optimum value for observing Ge atoms in the LIBS spectrum. It is possible to work with higher energy values of laser pulse and delay values for spectrometer but as described in A. Ceylan et,al [9] found that the thickness of the ZnO:Ge_Nr samples coating is approximately 900 - 1000 nm, and in light of this information with this much energy of the laser source it is possible to totally ablate the film and reach to the Si substrate.

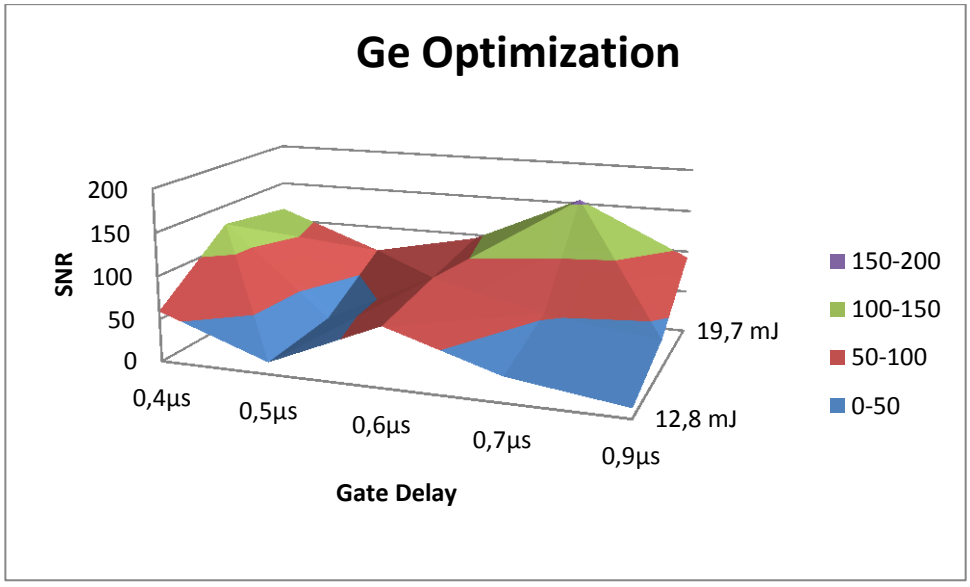

Figure 3.3 Optimization graph for laser energy and spectrometer delay time

It can be seen on the graph created by the depth profile data captured by the Bruker Dektak 150 model Surface Profiler in figure 3.4 that 9 consecutive shots of 19.7 mJ energy from the laser source is resulting with a creation of nearly 50 µm of crater, which means single shot will create more than 5 µm of crater on the thin film surface. Dektak 150 model profiler has the capability of sample measurement up to thickness 90 mm; it can perform a single scan of 55 mm. It has 100 x 100 mm measuring stage with full x-y motorization. Device has low-inertia sensor (LIS3) as stylus with 1mg to 15 mg stylus force. It is also sufficient for my requirements with its 1 mm vertical range and 0,1 nm vertical resolution

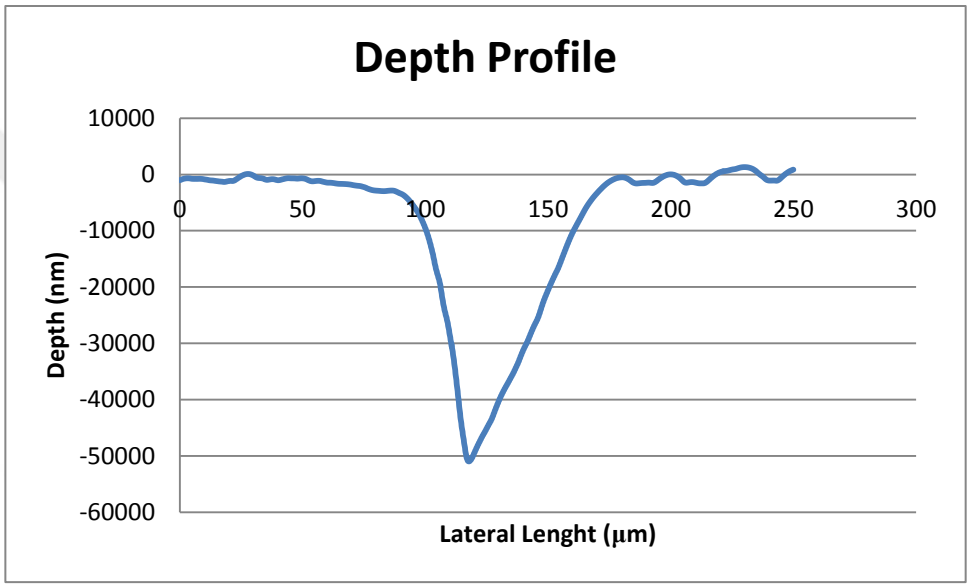

Figure 3.4 Depth measurement of crater created by 19,7 mJ Laser pulse

It is also a useful information to have the images of the sample under microscope after ablated with 19,7 mJ laser pulse as given in figure 3.5 below;

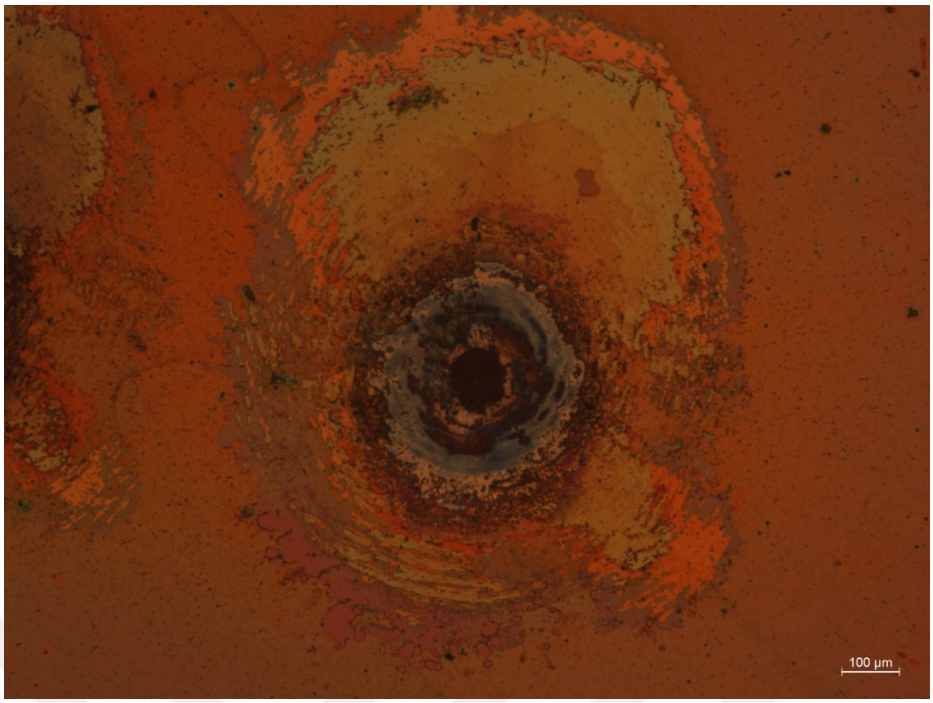

Figure 3.5 Microscope image of the crater formed on the film surface with 19,7mJ laser pulse energy.

So in this study optimizing the data would not be based on SNR, instead it will be more likely to be decided on spectrum data, means the lowest energy of the laser that Ge spectrum line can still be observed on the spectrum should be taken as data collection energy for the rest of the study.

3.4 RSTD calculation for the LIBS Setup

Relative standard deviation of the setup need to be calculated in order to understand the error coming from the system itself. This error is coming because of; the surface of the sample is distributed so that the focal spot of the laser is not same for each consecutive laser pulse and due to changing media conditions (varying particles present in front of the sample) in every shot, the absorbed partition of the laser beam is changing accordingly. Both these factors causes shot by shot fluctuations and poor reproducibility of the LIBS data. Wisbrun et. al study on different samples for relative standard deviation. [28] by using the RSTD calculation equation as below;

$$\text{RSTD} = (\text{Standard Deviation} / \text{Mean}) \times 100$$

A powder pellet formed from a %100 Ca sample is used. And by using the Ca 393,36 nm spectral line RSTD of the system with different energy levels of the Laser pulse is calculated. Calculated values are shown on the table 2.

Table 2 RSTD calculations with different laser energies and 0,7 μs gate delay

Laser Pulse Energy	Area Under Ca Peak (mean)	STD	RSTD
11,2 mJ	348218.45	58441.45	17%
12,8 mJ	413815.6	66322.24	16%
16,7 mJ	474989.75	54925.95	19%
19,7 mJ	769336.35	16.027	7%

3.5 Structural Analyses of ZnO:Ge Thin Film Samples

The system explained in "LIBS Experimental Setup" is used to collect spectral data from ZnO:Ge samples. It is known that using higher energies of laser pulses it is not possible to get any information from the Zn and Ge coated layers in the samples instead all energy transferred to the films is causing a total ablation of the film and reaching to the Si substrate at the very first plasma initiation. With the light of this experience lower energies of laser pulses are used to collect data from the samples to get as much information as one can get. At the lowest possible energy by increasing the Q-Switch delay of the laser source which is inversely proportional with the pulse energy created.

Spectrum lines observed from Ge atoms with system arrangement as; the 270 μs delay for Q-switch, which corresponds 10 mJ pulse energy and 0,7 μs gate delay as it was already proved by the optimization study in the beginning of the data collection. Ge lines are used to decide the lowest energy required as because, it is the crucial species in the film as it is doping element between the ZnO layers and also transition probability of Ge element is way lower than the other species in the target like Zn and Si.

Spectrum data collected from samples of ZnO:Ge thin film with different processed as described in the "Preparation of ZnO:Ge nano composite thin film" section of this study. Pictures of the samples prepared after data collected can be seen in figure 3.6.

a)

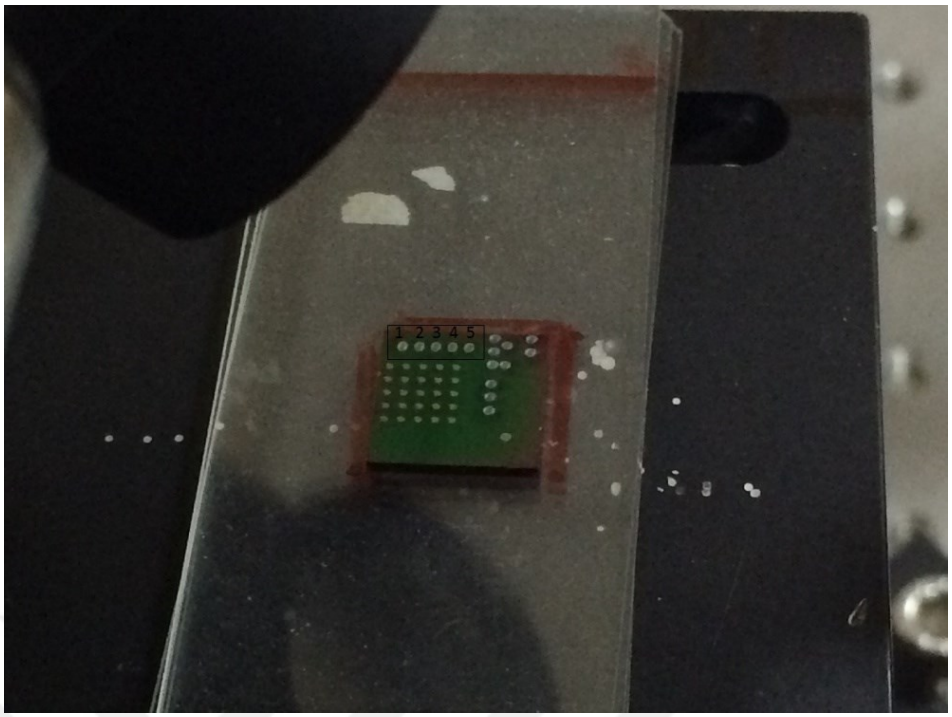

b)

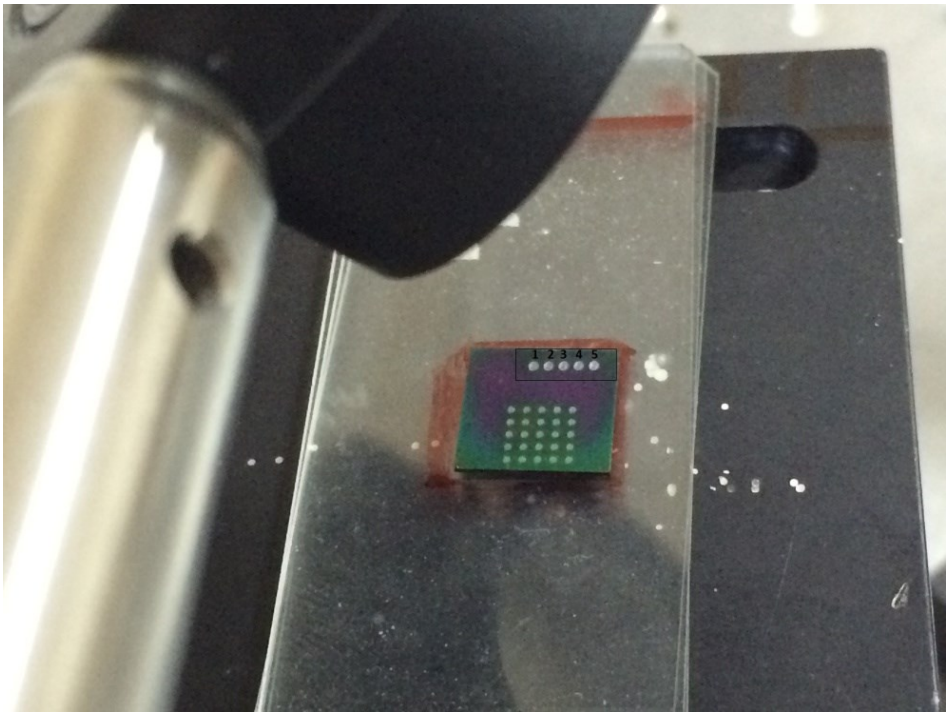

c)

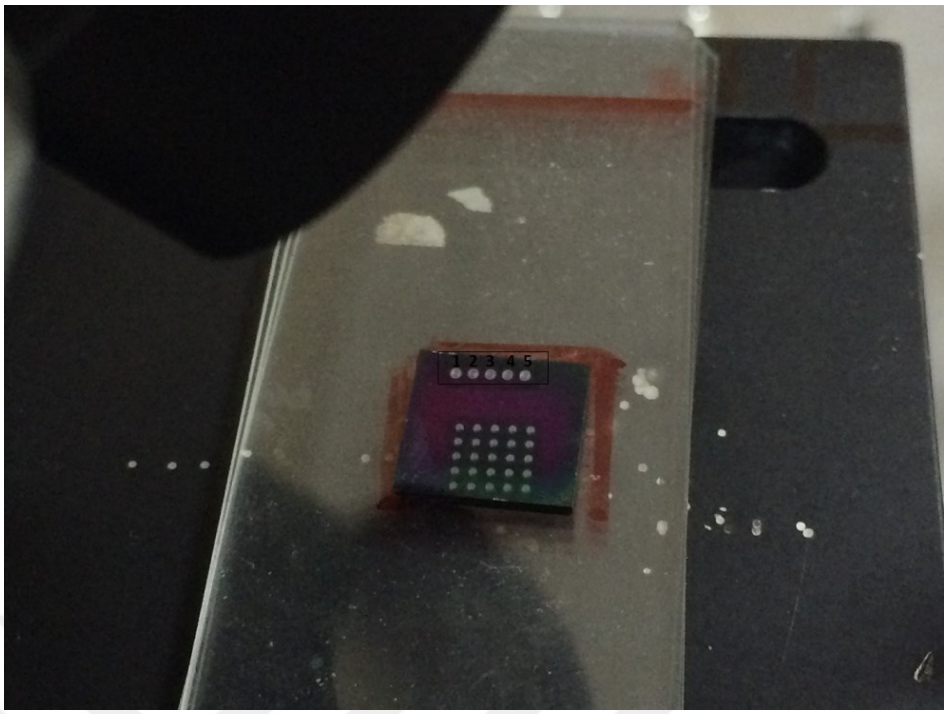

d)

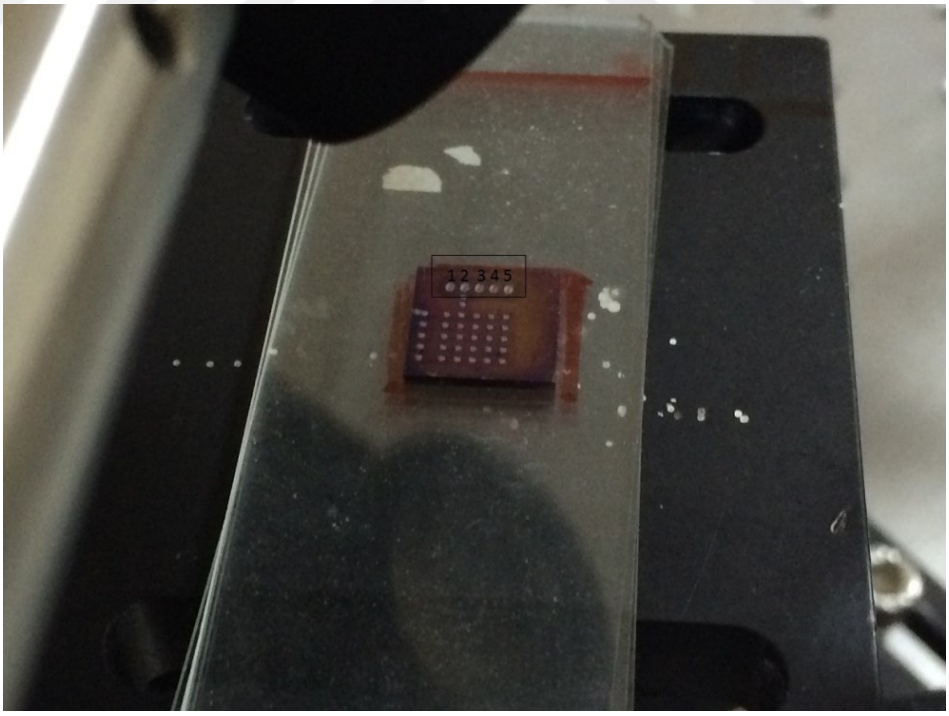

Figure 3.6 Sample photos; a) ZnO:Ge_1m b) ZnO:Ge_1m_30s c)ZnO:Ge_1m_60s d)ZnO:Ge_1m_90s

Photos are showing the samples just after data collected with producing laser plasma on 5 different locations of each sample. 30 consecutive laser pulse shots are applied to every location. Locations are indicated on the pictures with the numbers given according to the shot queue. Craters formed on the samples are created by using; 250 µm pulse diameter, 4nm pulse width and 10 mJ laser energy of New wave 50 mJ Nd:YAG laser with 0,7 µs spectrometer gate delay of Aurora 5 channel spectrometer.

Below table is giving the spectrum lines of each species in the samples which are Zn, Ge and Si. Data is examined over TruLIBS wavelengths of the elements. It is also studied from the same lines by Şerife et.al for Ge and Si. [10]

Table 3 NIST & TruLIBS Atomic Spectrum Lines

	NIST Atomic Spectrum Database	**TruLIBS Database**
Element	Spectral Line Wavelengths	Most Intense
Zn	481,053 nm - 472,215nm	481,053 nm
Ge	326,94 nm - 306,70nm - 303,90nm	303,90 nm
Si	288,15 nm - 390,55 nm	390,55 nm

Spectrum graphs are showing the lines of inspected elements in the samples below, as the Ge is disappearing in the spectrum after 4^{th} shot and the Zn after 10^{th} – 12^{th} shots accordingly in different samples only 15 shot data is investigated plotted on the graph.

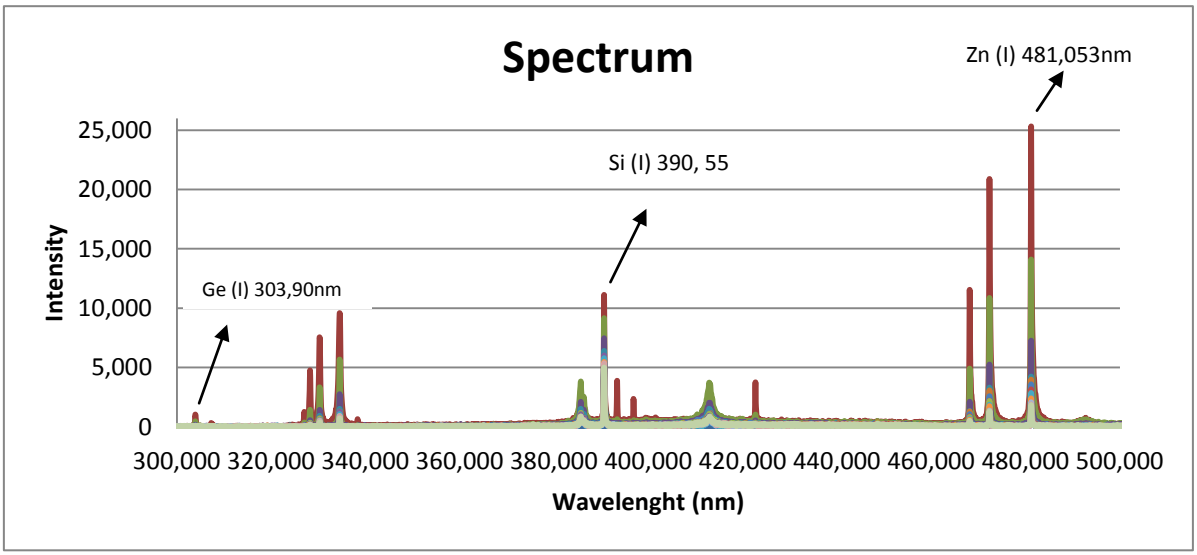

Figure 3.7 Spectrum data from 15 consecutive shots from ZnO:Ge_1min_asmade_Nr

As seen in the figure 3.7 relative intensities of the species in the sample are having so high difference, in magnitudes as related to their emission probabilities and the

properties of the spectrum and detector used. As we are working for structural analyses of the samples by using the LIBS spectrum data, we need to understand the location and shot dependant behavior of each element we are investigating.

In order to study the behavioral differences if there will be any, than one should plot the area under peak of each interested line in the spectrum and draw the data with location and shot number depended for each species and then this picture should be discussed according to process types of samples. Figures 3.8, 3.9, 3.10 and 3.11 below are the graphs plotted accordingly;

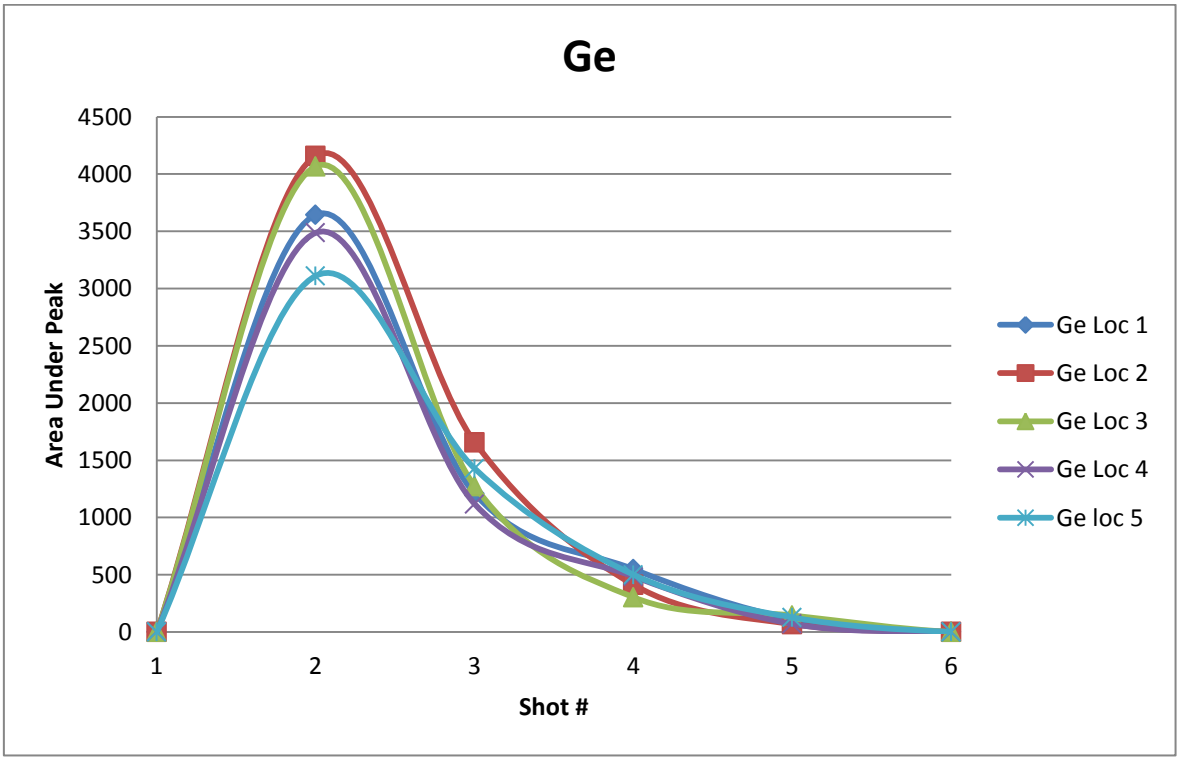

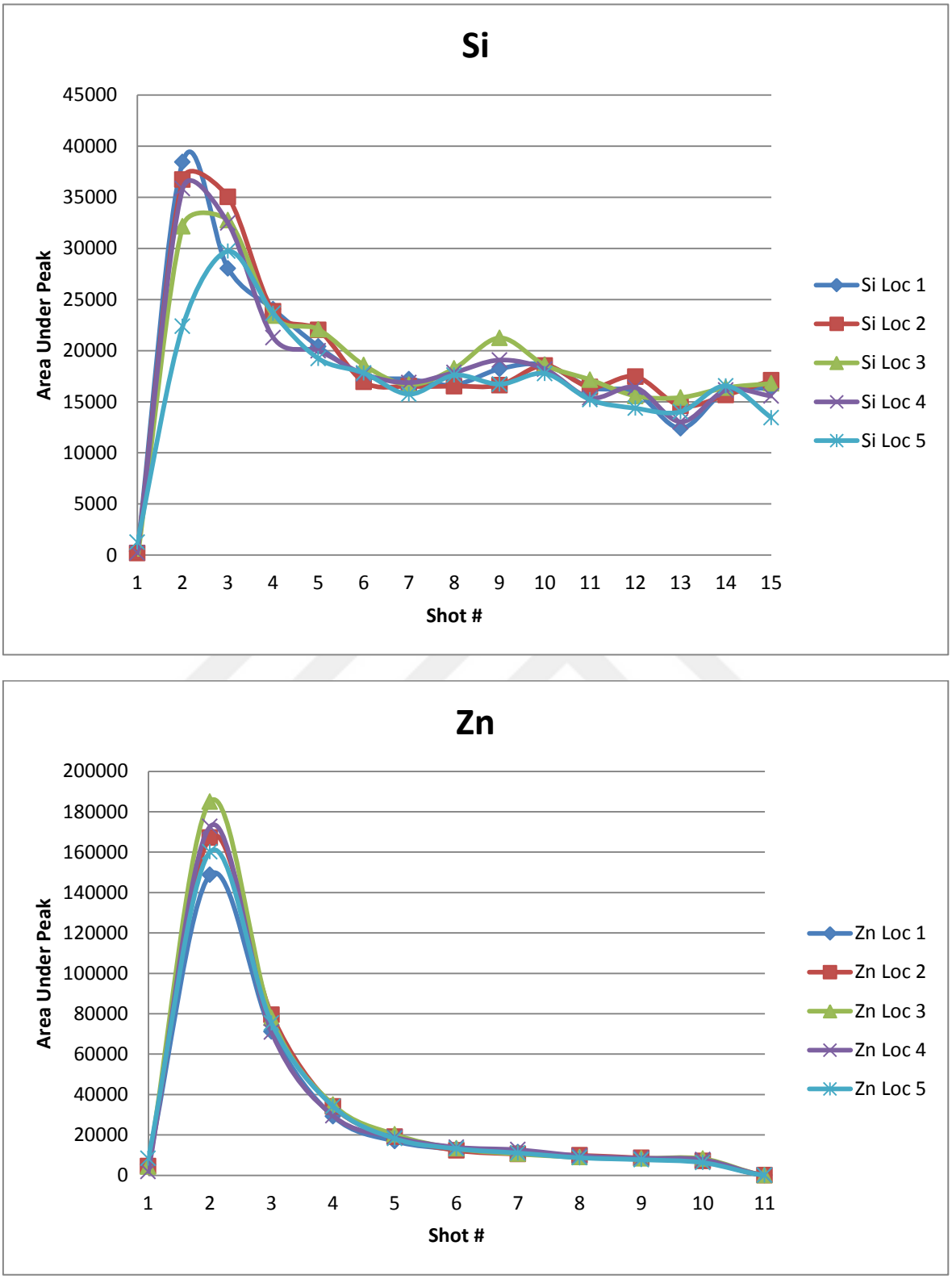

Figure 3.8 Area under peak against shot #, location depended (ZnO:Ge_1min_asmade_Nr)

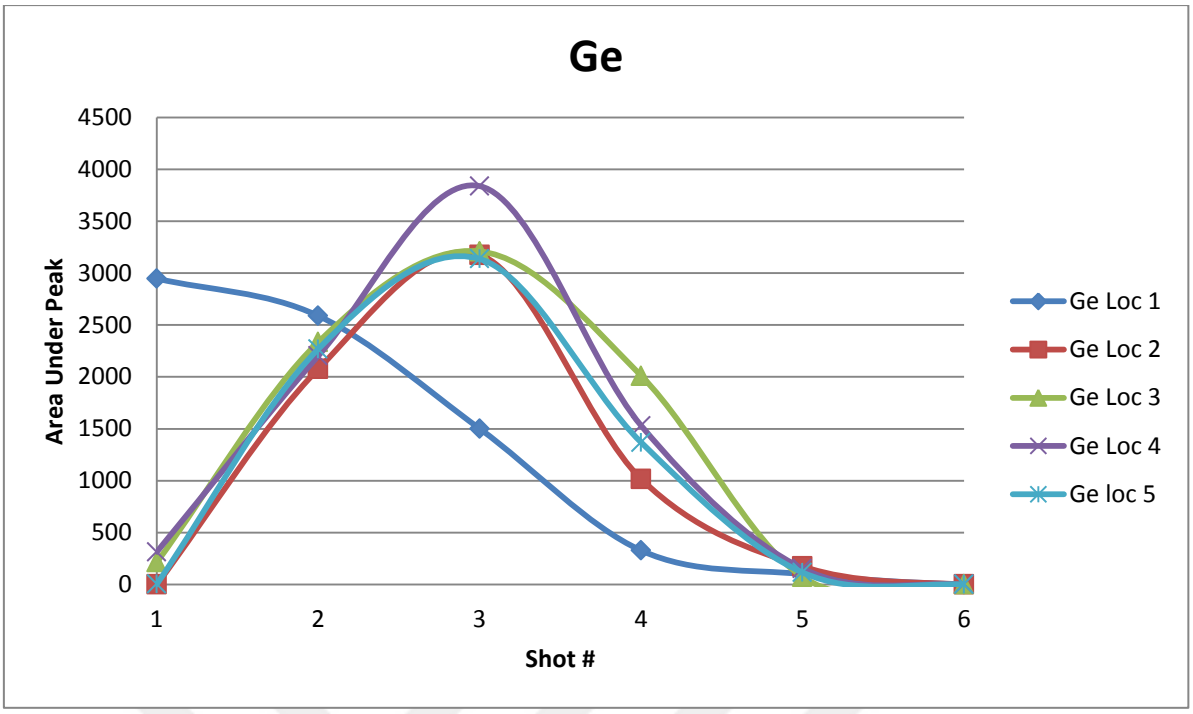
Ge
4500
4000
3500
3000
2500
2000
1500
1000
500
0
Area Under Peak
1
2
3
4
5
6
Shot #
Ge Loc 1
Ge Loc 2
Ge Loc 3
Ge Loc 4
Ge loc 5

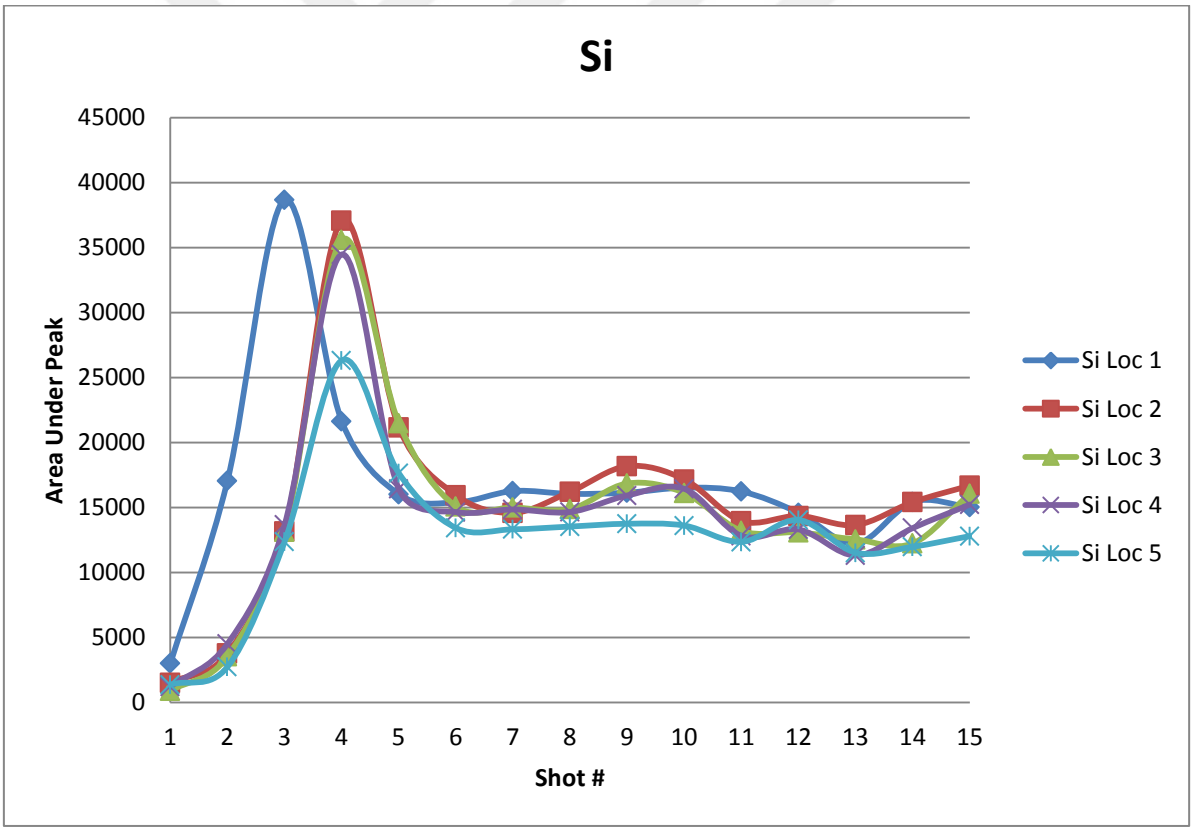
Si
45000
40000
35000
30000
25000
20000
15000
10000
5000
0
Area Under Peak
1
2
3
4
5
6
7
8
9
10
11
12
13
14
15
Shot #
Si Loc 1
Si Loc 2
Si Loc 3
Si Loc 4
Si Loc 5

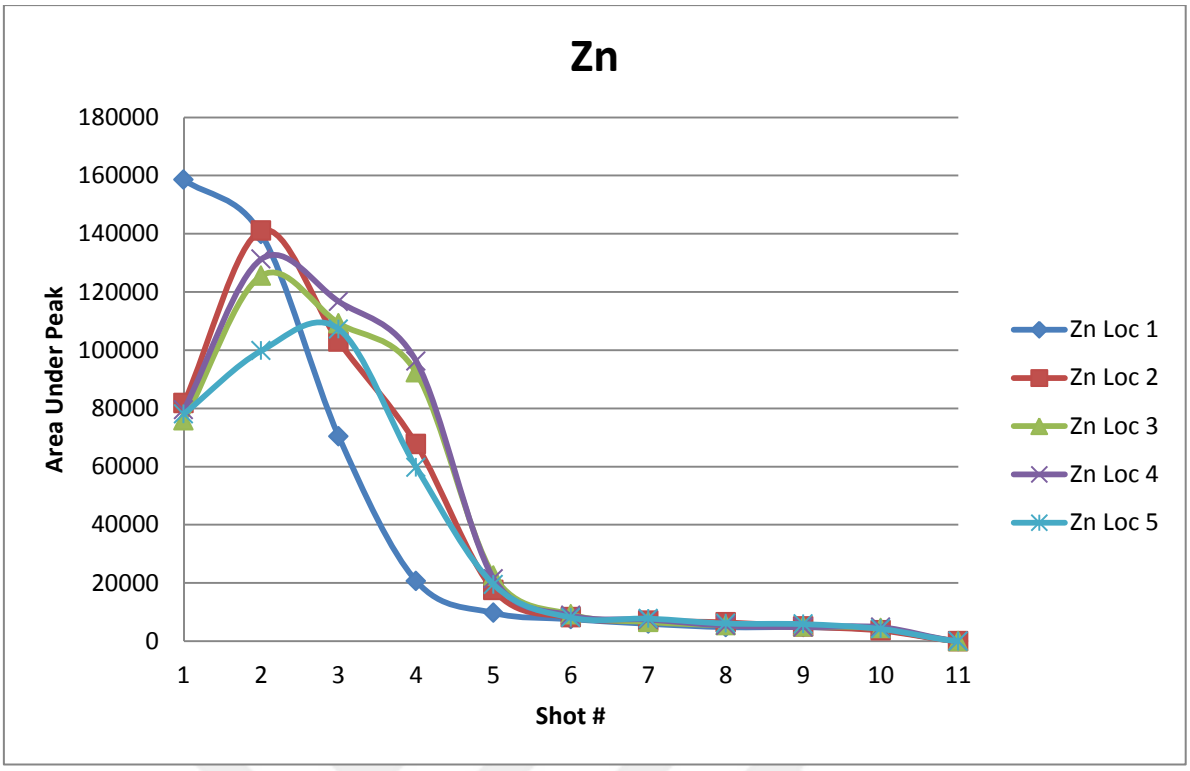

Figure 3.9 Area under peak against shot #, location depended (ZnO:Ge_1min_30s annealing_Nr)

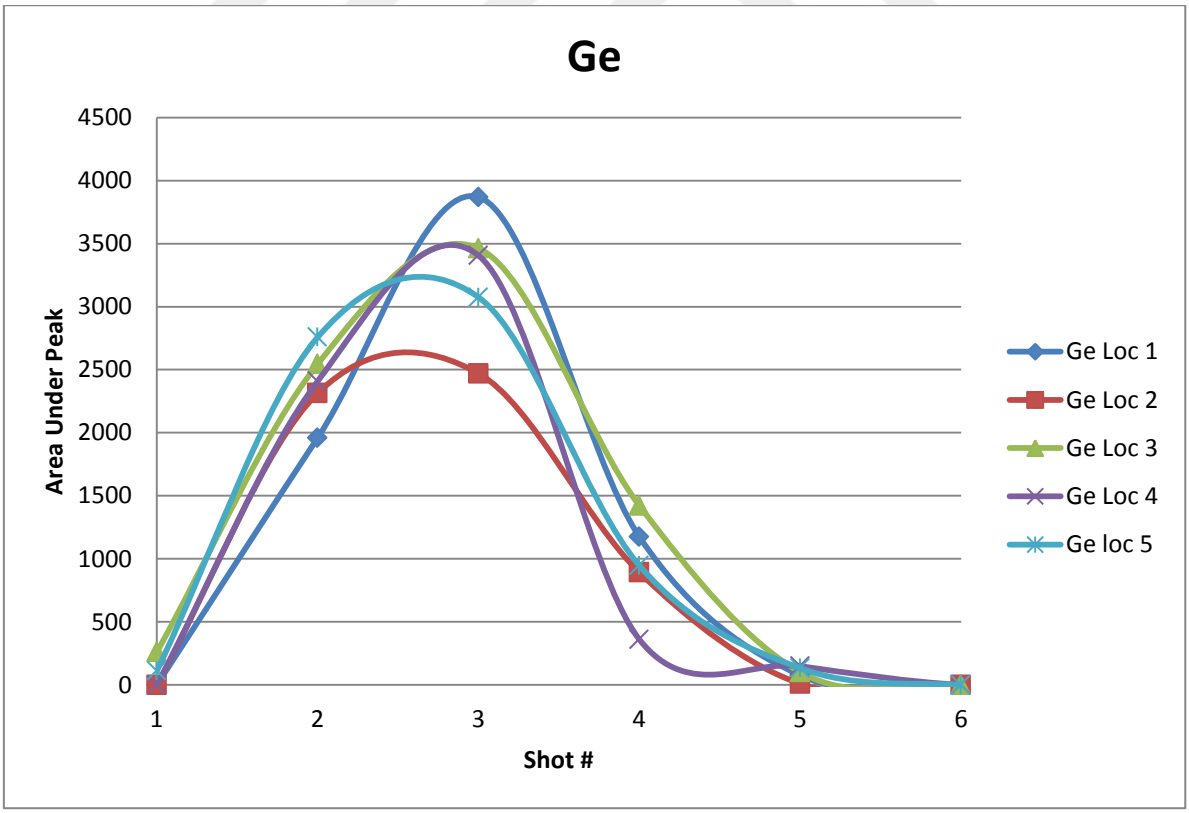

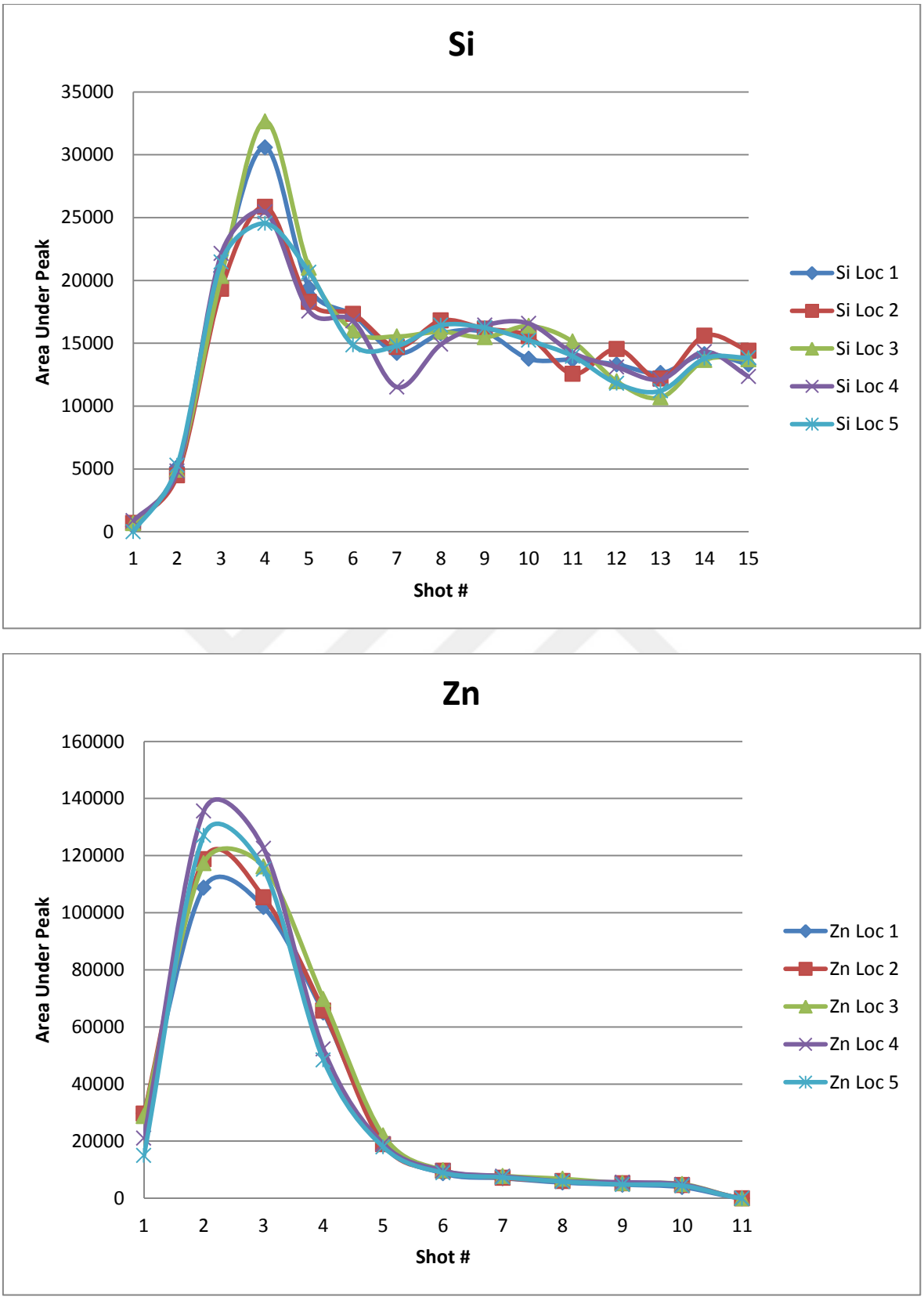

Figure 3.10 Area under peak against shot #, location depended (ZnO:Ge_1min_60s annealing_Nr)

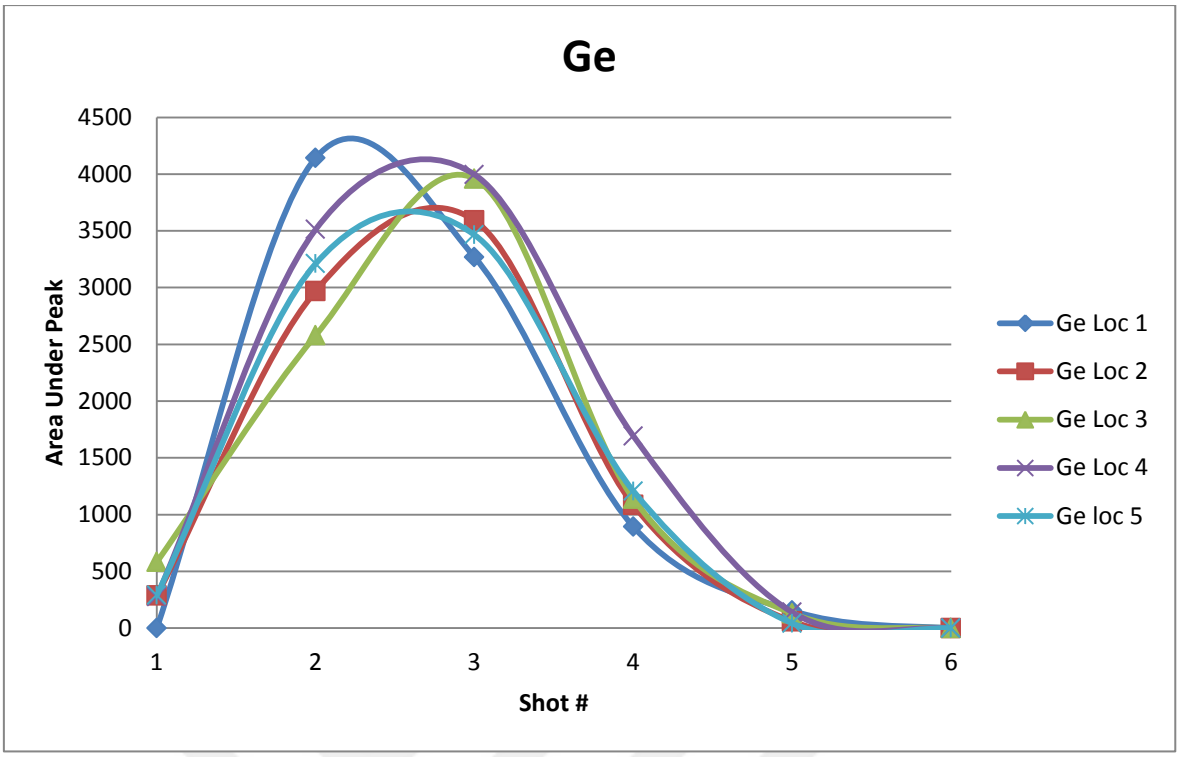
Ge
4500
4000
3500
3000
2500
2000
1500
1000
500
0
Area Under Peak
1
2
3
4
5
6
Shot #
Ge Loc 1
Ge Loc 2
Ge Loc 3
Ge Loc 4
Ge loc 5

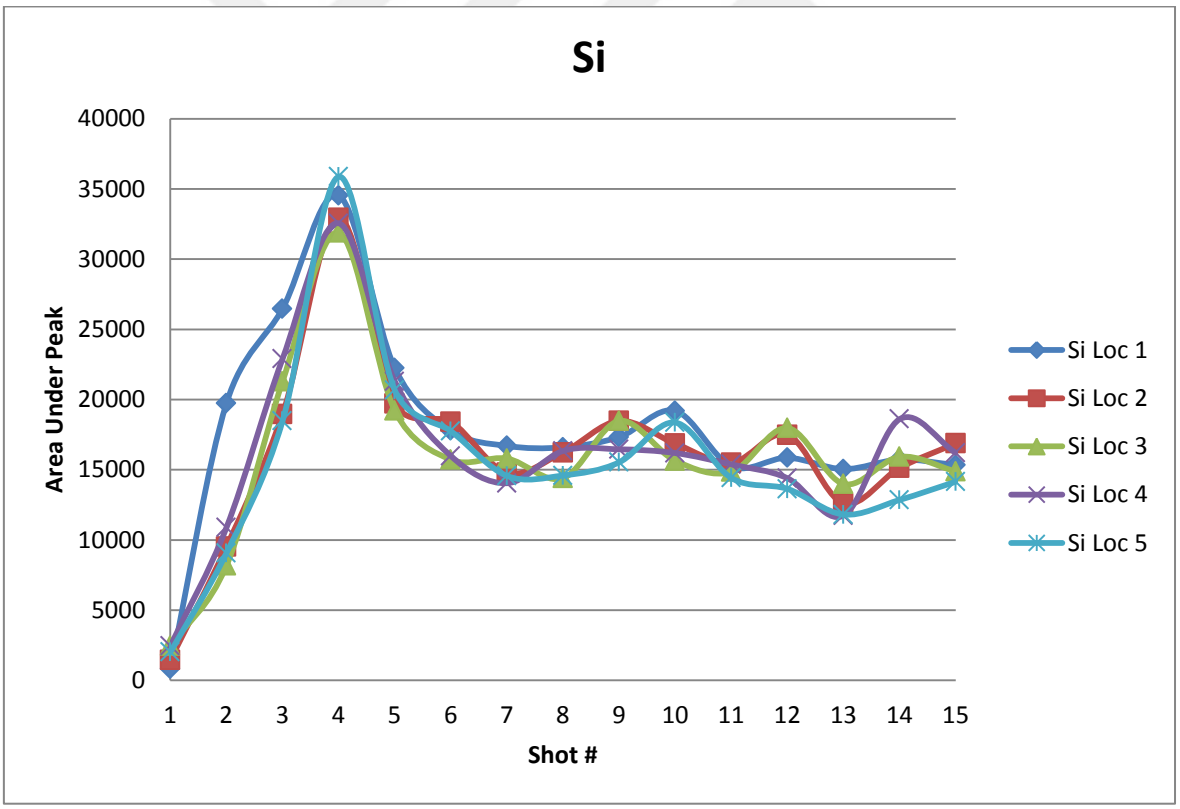
Si
40000
35000
30000
25000
20000
15000
10000
5000
0
Area Under Peak
1
2
3
4
5
6
7
8
9
10
11
12
13
14
15
Shot #
Si Loc 1
Si Loc 2
Si Loc 3
Si Loc 4
Si Loc 5

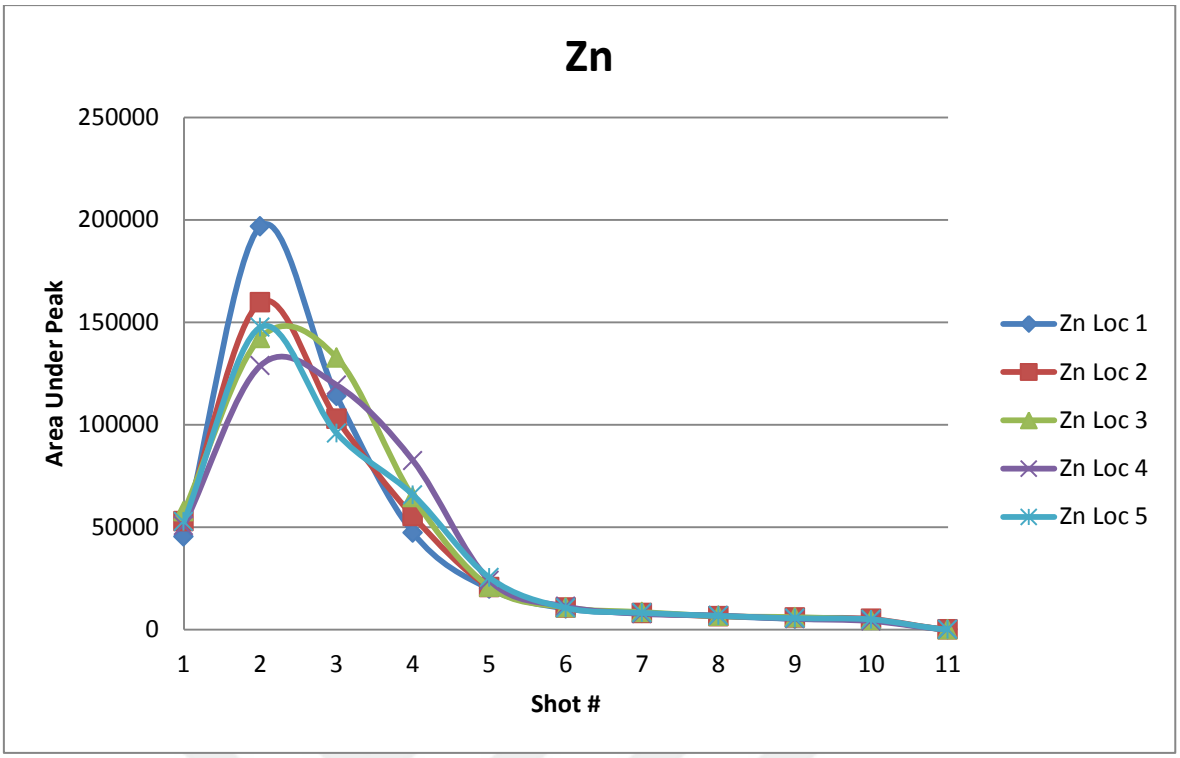

Figure 3.11 Area under peak against shot #, location depended (ZnO:Ge_1min_90s annealing_Nr)

According to the graphs of all samples, it is obvious that Ge spectrum is starting to be visible on 2nd shot and vanishing after 4th shot of laser pulse. Zn is similarly behaving as Ge and starts to be present in the 2nd shots and vanishing in the 10th shot of laser pulse. If we come to the Si behavior, it is so much different than the other species and has a continuous presence in all consecutive laser shots with decreasing intensity after 4th shot. Such information is giving us a rough estimation for coating thickness of the samples, so one of the samples chosen (ZnO:Ge_1min_asmade_Nr) to be analyzed for depth profiling with Dektak 150 Surface Profiler. Microscope image of the measured sample is in figure 3.13. Data received from profile measurement is plotted on a graph seen below figure 3.12

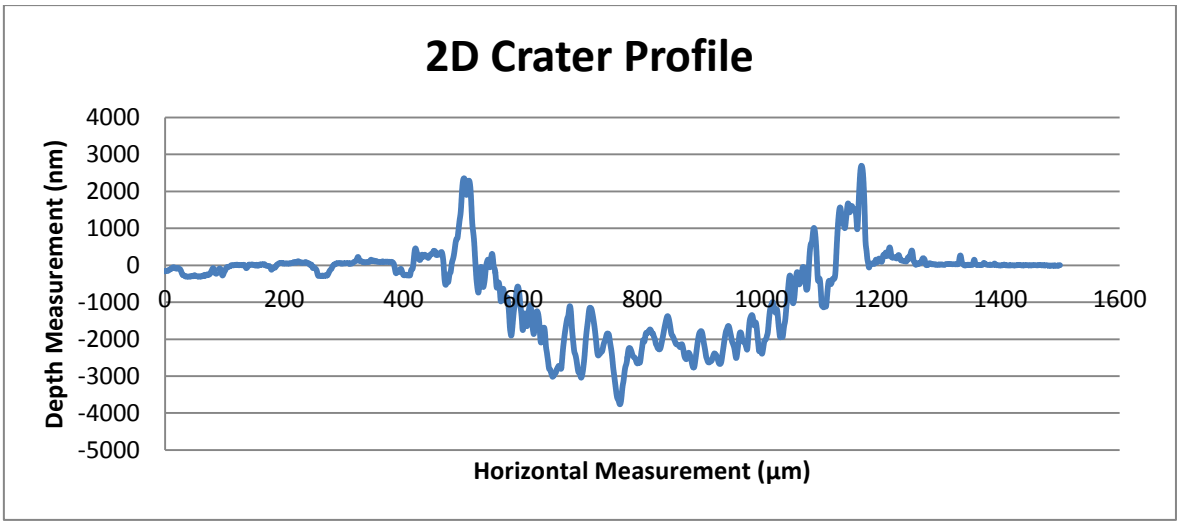

Figure 3.12 Depth measurement of a crater, formed on the sample surface after 30 consecutive laser shots. (Dektak 150 Surface Profiler)

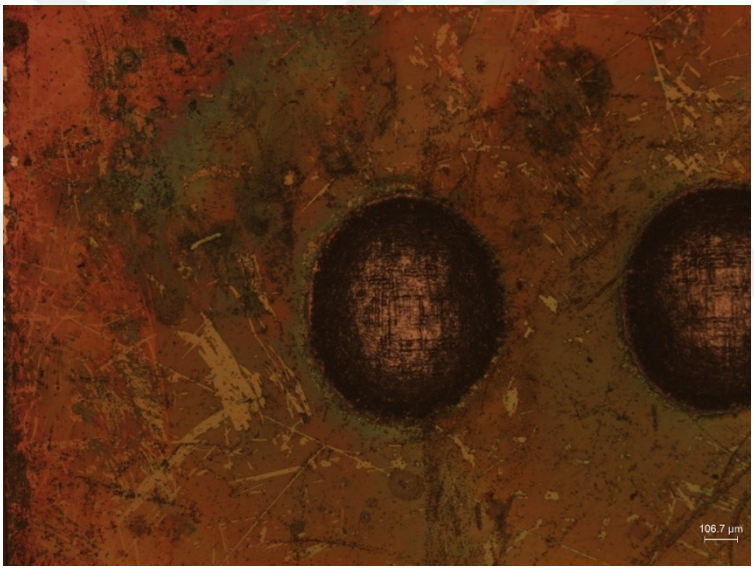

Figure 3.13 Microscope image of the crater after 30 consecutive laser shots

The maximum measured depth is 3.760 nm after 30 laser shots. Assuming the shot penetration depths are approximately equal to each other, it means as a rough calculation every single shot is ablating approximately 125 nm of film thickness.

On the other hand, this rough graphs of species depended on shot number and location, is not giving a sufficient idea to figure out the structure of the thin film coating and the surface homogeneity differences of the coating types. According to this, it would be needed to see the fluctuations of the intensity, location depended for Ge and Zn (Main components of the coating film) to have further knowledge on the structural composition of each sample.

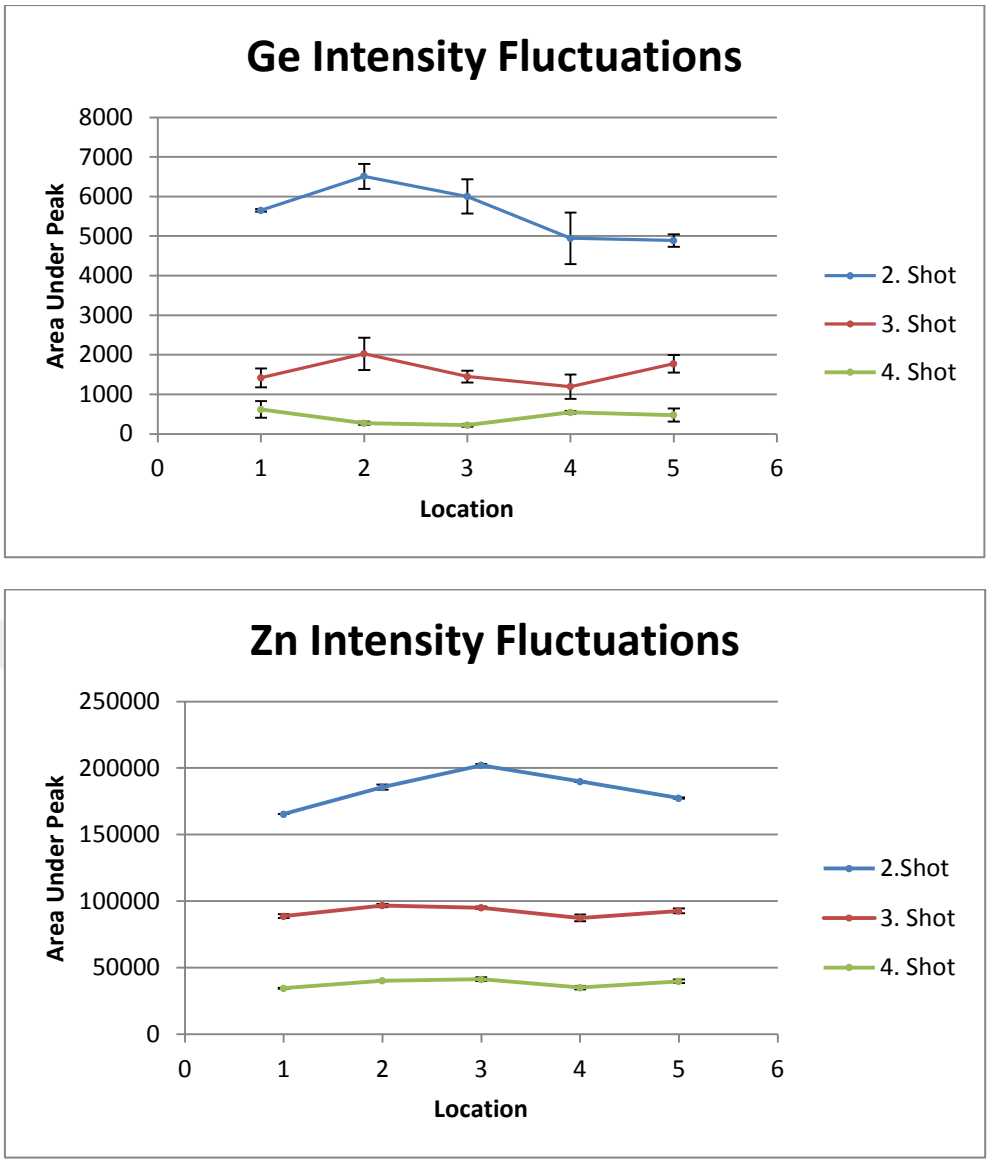

Figure 3.14 Area under peak fluctuations according to 5 different locations (Locations are on a straight line and 1mm distance each) (Sample ZnO:Ge_1min_asmade_Nr)

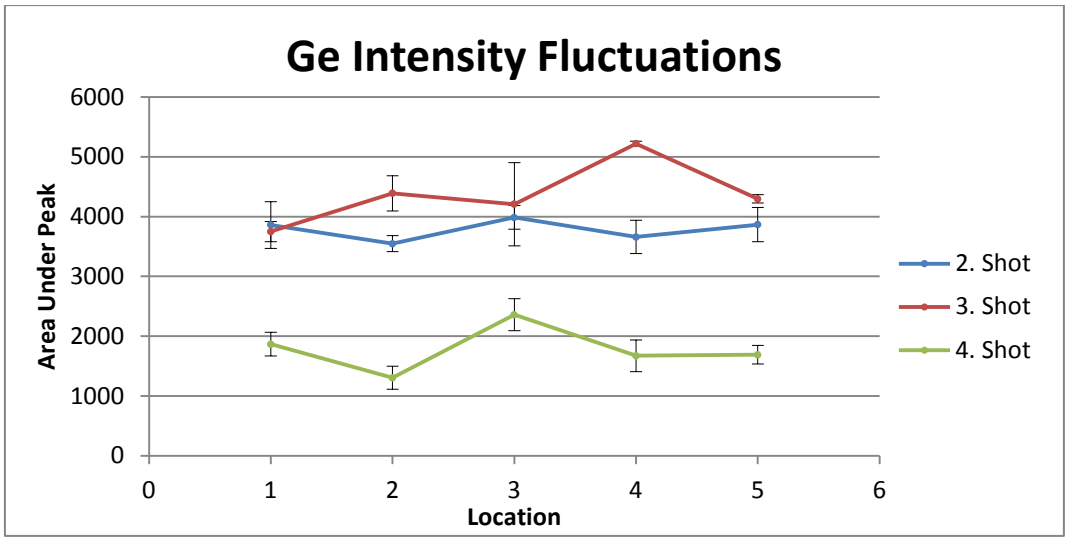

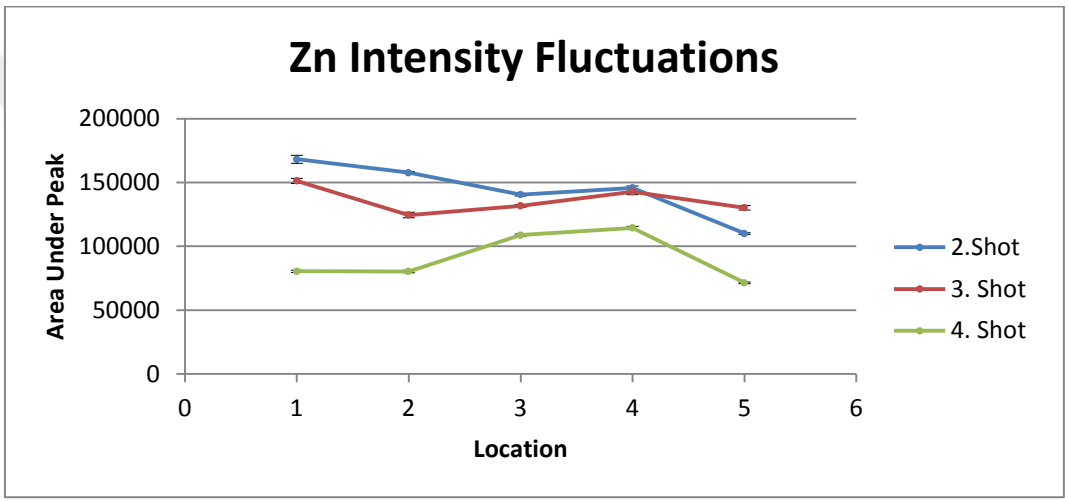

Figure 3.15 Area under peak fluctuations according to 5 different locations (Locations are on a straight line and 1mm distance each) (Sample ZnO:Ge_1min_30s_Nr)

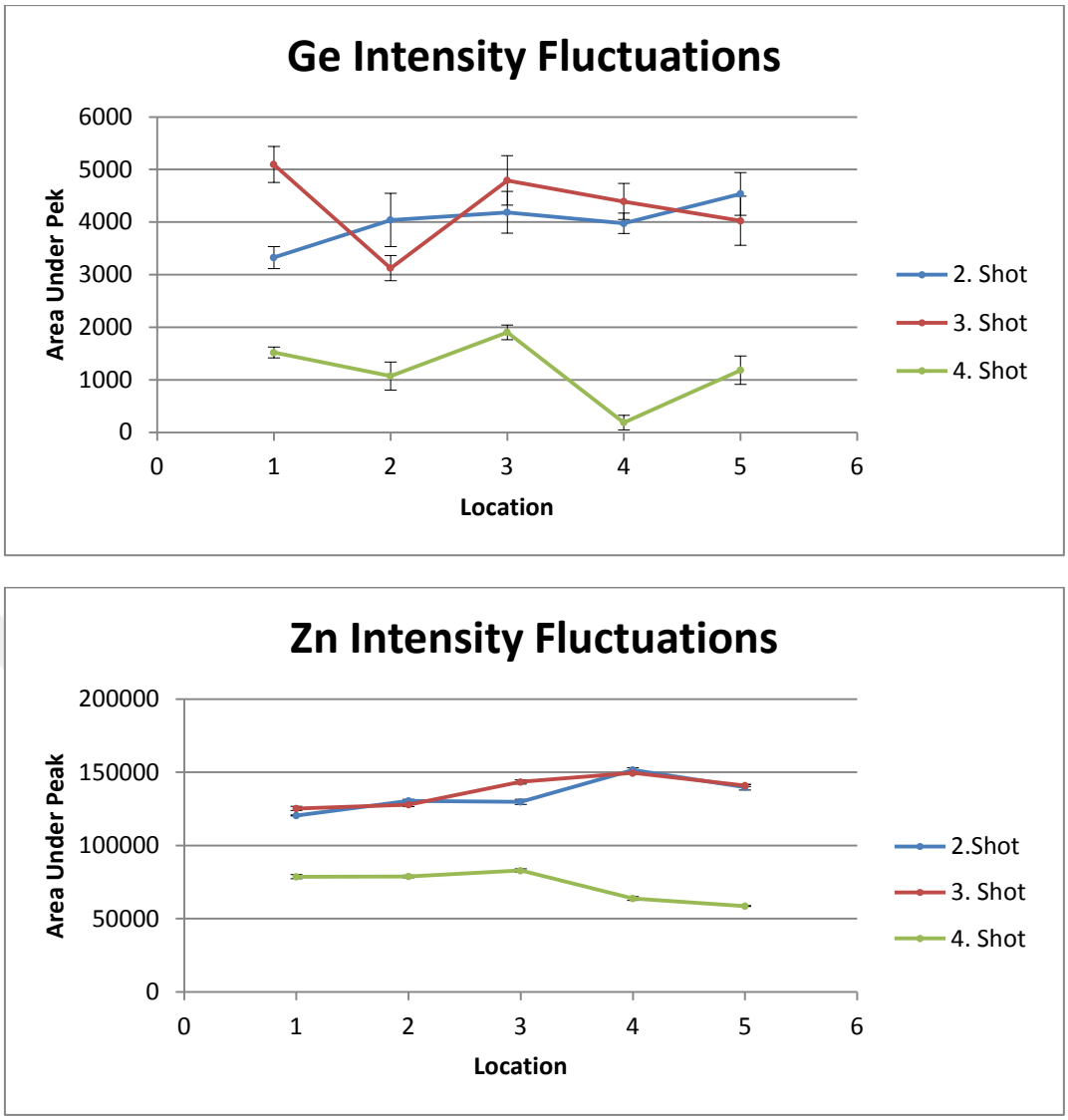

Figure 3.16 Area under peak fluctuations according to 5 different locations (Locations are on a straight line and 1mm distance each) (Sample ZnO:Ge_1min_60s_Nr)

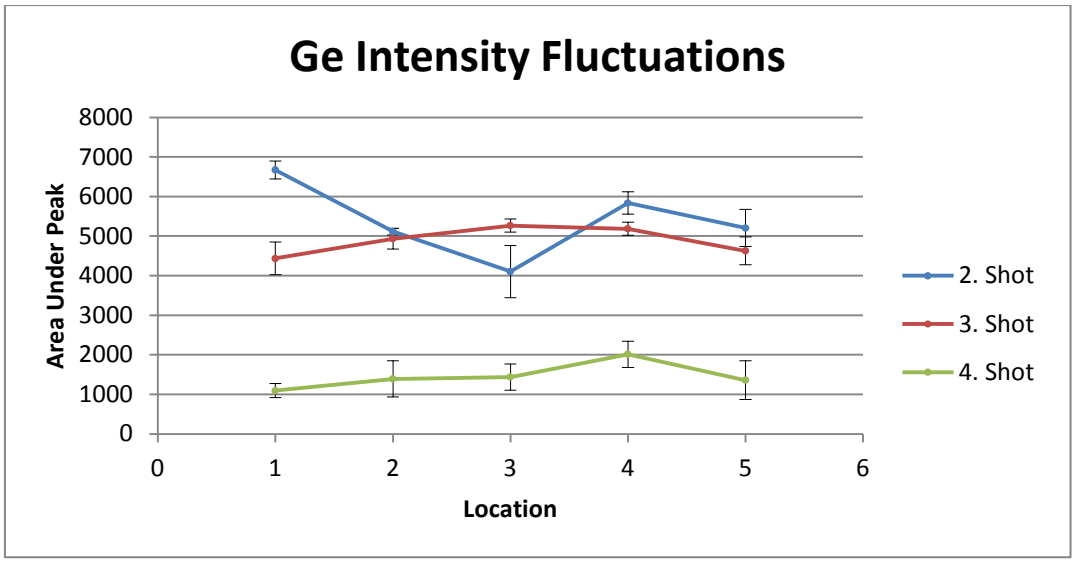

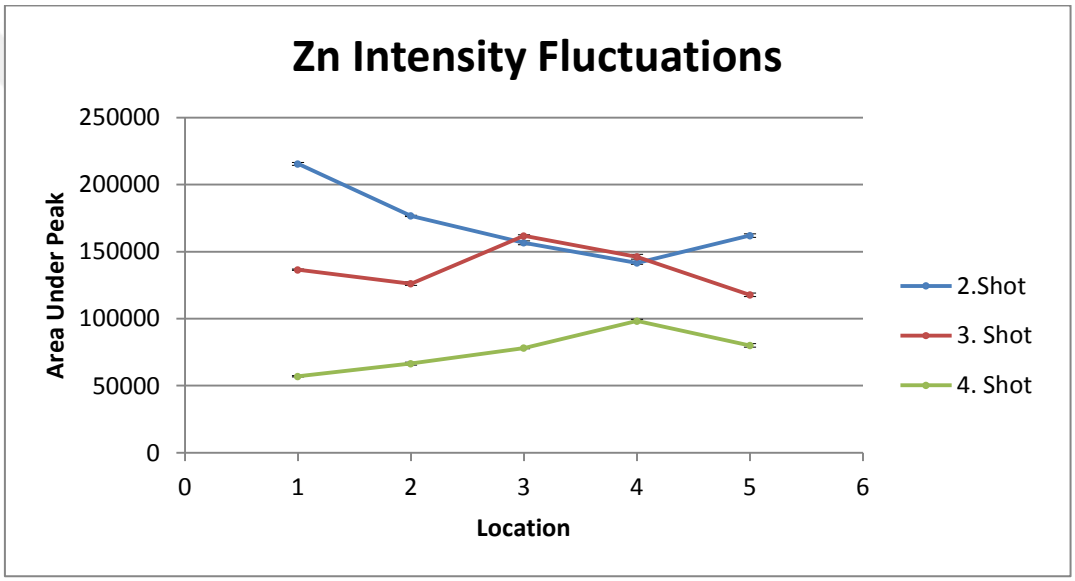

Figure 3.17 Area under peak fluctuations according to 5 different locations (Locations are on a straight line and 1mm distance each) (Sample ZnO:Ge_1min_90s_Nr)

Because of the nature of LIBS, shot to shot error will differ from each other. Main contributor of this error is the background noise in the spectrum of the plasma created. LIBS is an in-situ analyzing technique, meaning that there is no need for a preparation of special environmental conditions for the sample to be investigated. On the other hand this quick and easy way of data measurement brings environmental errors in every single spectrum data taken from the sample and every error would be way different than the other. As the system is open to atmospheric conditions and the plasma is created in the air, it is obvious that in every single plasma created, there will be other accompanying species

in different concentrations in the air just in front of the target. Secondly, as the laser pulse is ablating the target surface in every single shot, the shape of the target surface area is changing. Due to this change, laser energy absorbed by the sample is changing shot by shot as well. To avoid the error coming from every shot, SNR (Signal To Noise) is calculated by the below equation for every spectrum line observed;

SNR = STD Baseline Fluctuation / Max. Intensity

Than SNR derived from above method are used to give the error on every spectrum data by error bars. SNR values are bigger in Ge spectra lines than Zn because the intensity of the Ge lines are so much lower than the Zn spectrum lines. So background noise is dominating Ge signal much more than the Zn signal.

4. Results and discussion

To understand the structural information received from the LIBS data, it is needed to compare them with the other structural analyses techniques such as XRD, SIMS and SEM. As these samples are already studied in mentioned structural analyses in various studies [9], [25], [27], one should compare the results of LIBS data with those study results.

Ceylan et, al stated in his study [9] about differences in thin film formation between absence and presence of O^- ions during the sputtering process of Zn and Ge ions on the Si substrate and named it as non-reactive sputtering and reactive sputtering process. It is valuable information to understand that, while formation of the Zn and Ge layers, oxidation effect of O^- ions presence in the sputtering is affecting the thickness of the whole film created. This can be explained by ZnO grain growth in the non reactive samples seems to be happening very loosely packed compared to the ZnO grain growing in the reactive samples. Also it is known that [9], because of loose formation of ZnO grains, inter diffusion of Si atoms are observed in non-reactive samples in the SIMS results, contrary no Si atom signal can be observed with the reactive grown samples due to close packed formation of ZnO grains are not letting the intra free spaces for Si atoms to diffuse in the layers of the ZnO and Ge. Differences mentioned above are seen in the figure 4.1 received from SIMS and SEM results for ZnO:Ge_60s reactive and non-reactive next to each other [9]

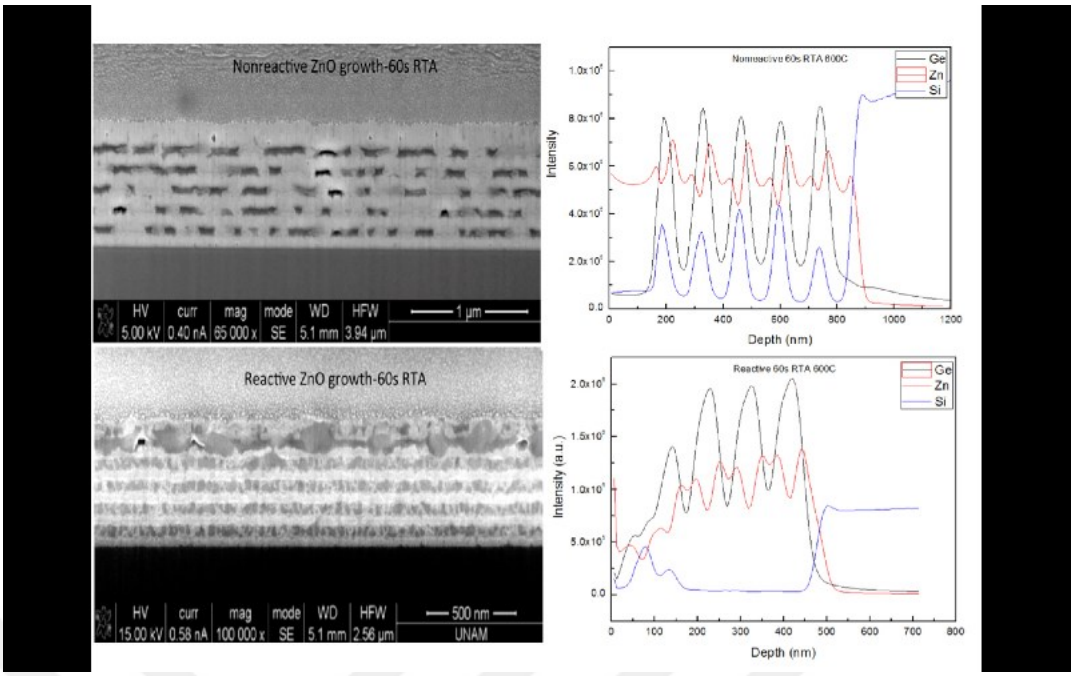

Figure 4.1 SEM data from cross section of ZnO:Ge_60s samples on the left for reactive and non-reactive. SIMS intensity – depth graphs of the same samples on the right

We also know that there are significant structural differences between the samples having different RTA (Rapid Thermal Annealing) timings and also between the one and the others that is remained as prepared without any RTA process. Annealing process applied to ZnO:Ge thin films is mainly acting on the Ge atoms and resulting in crystallization of Ge in diamond cubic or simple tetragonal phase (ST12Ge) in some certain specific conditions [29], [30]. Figure 4.2 – 4.7 is showing the SEM images of the samples of ZnO:Ge thin films as described above;

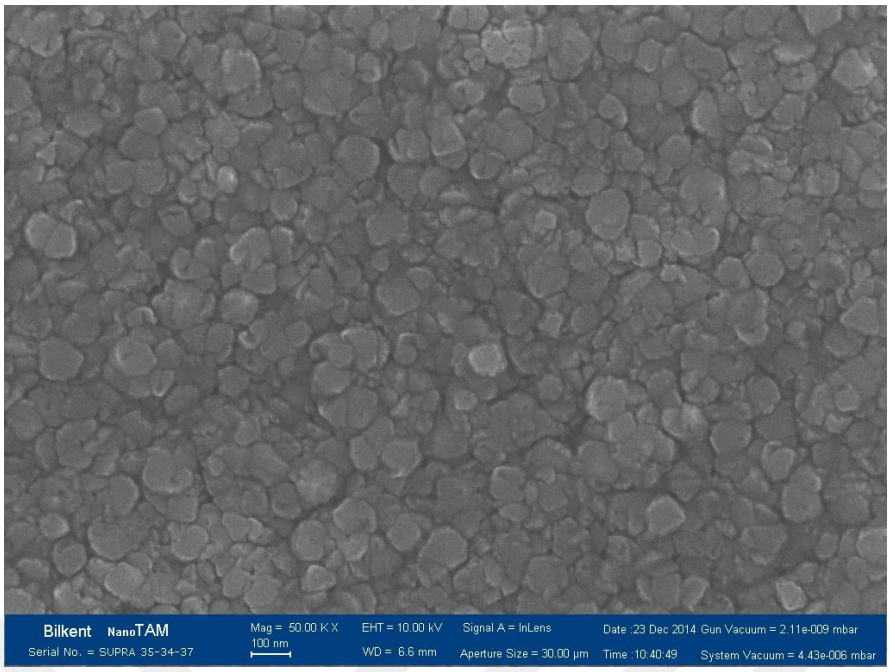

Figure 4.2 SEM Image showing the surface (ZnO:Ge_asmade_Nr)

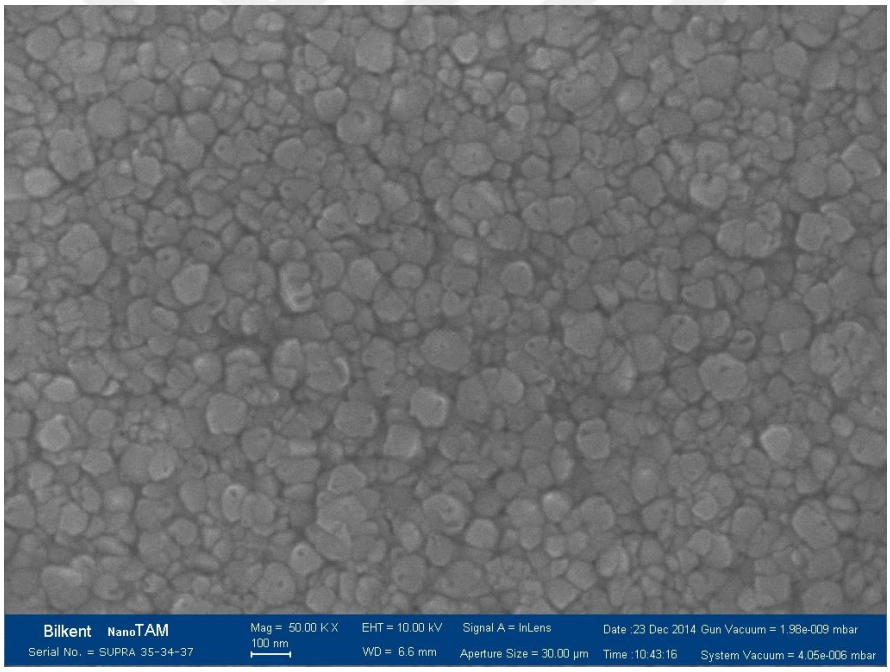

Figure 4.3 SEM Image showing the surface (ZnO:Ge_30 s_Nr)

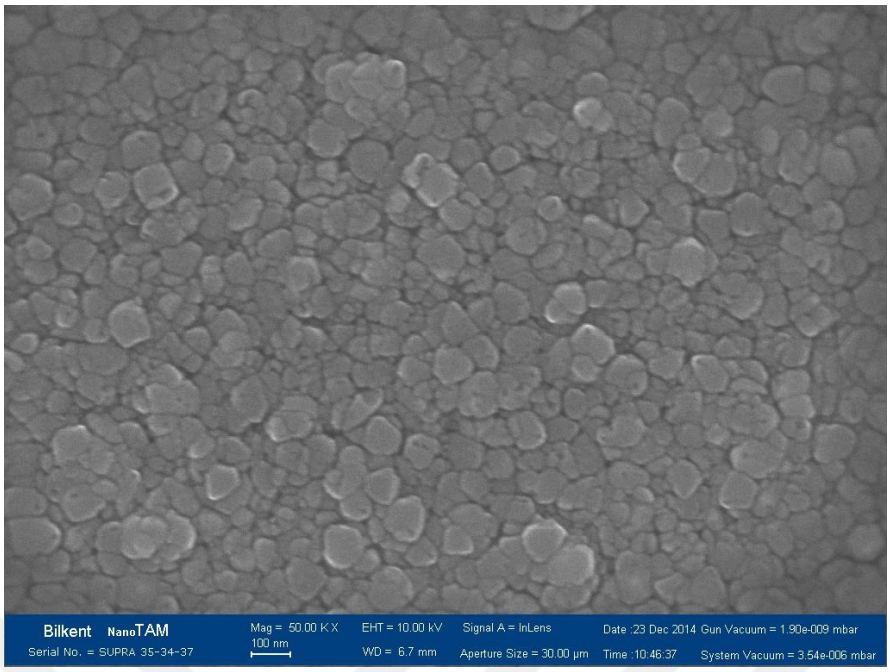

Figure 4.4 SEM Image showing the surface (ZnO:Ge_60 s_Nr)

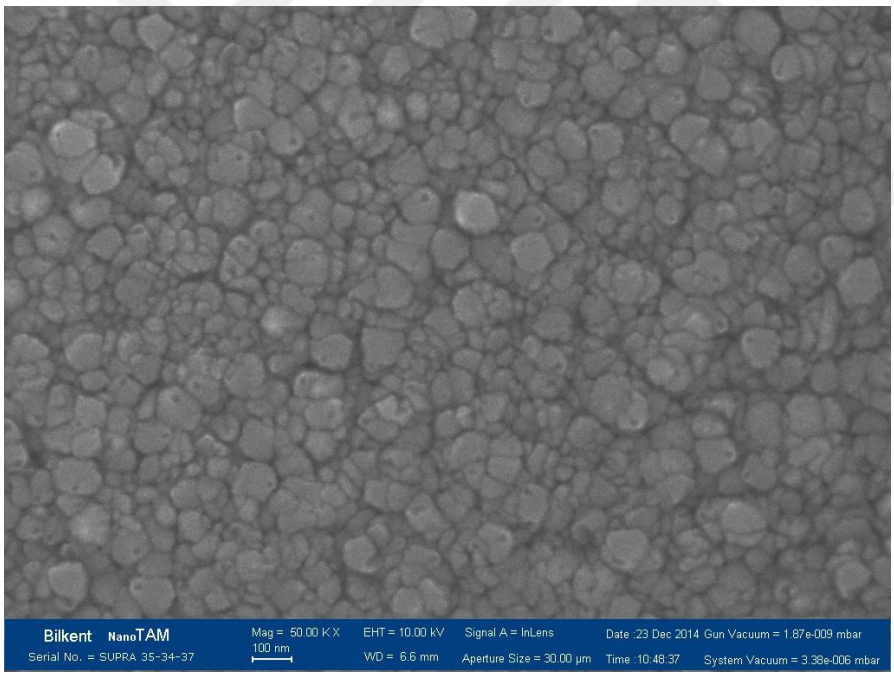

Figure 4.5 SEM Image showing the surface (ZnO:Ge_90 s_Nr)

It will be also valuable to have the cross sectional images of the samples in order to understand the layer formation as mentioned before. Below SEM images are showing the cross sectional area of the samples.

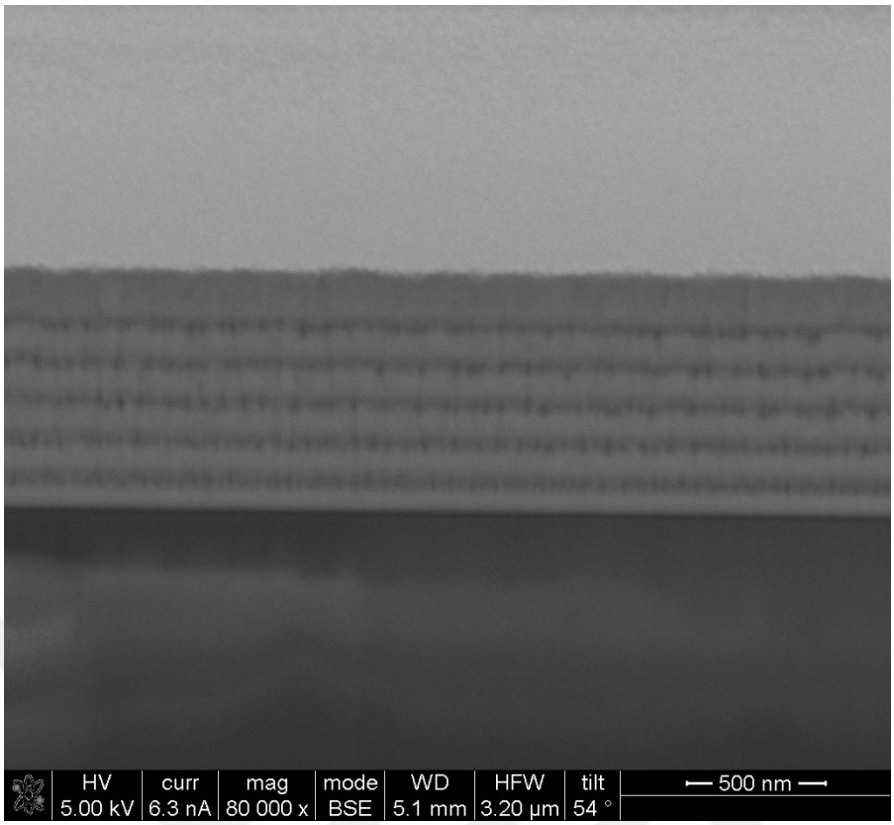

Figure 4.6 XSEM Image showing cross section (ZnO:Ge_asmade_Nr)

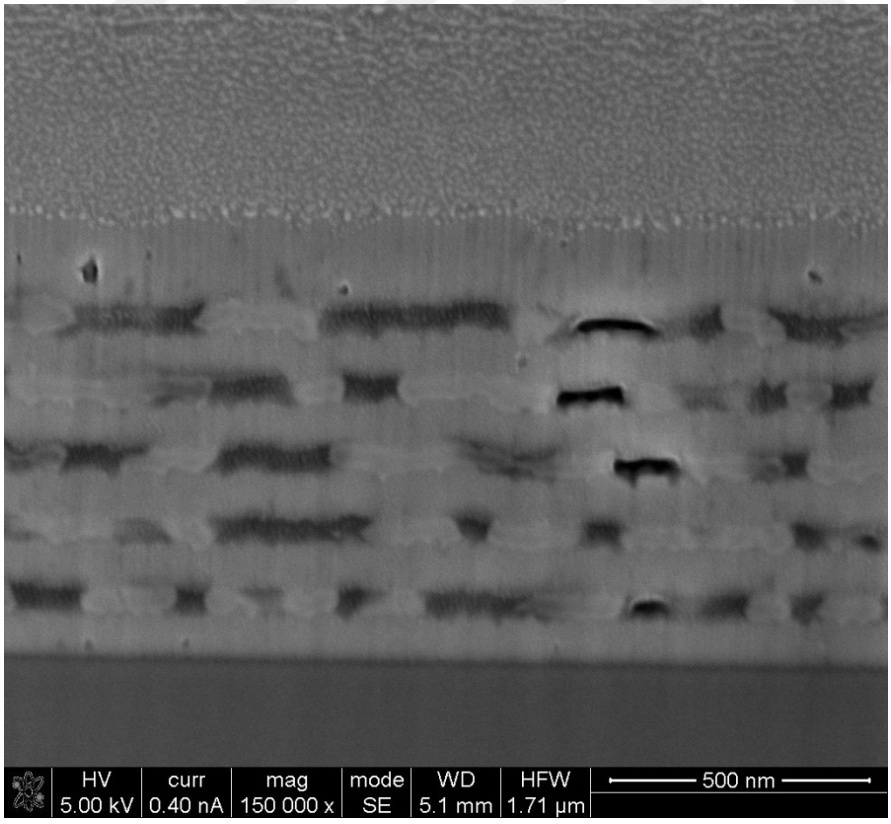

Figure 4.7 XSEM Image showing cross section (ZnO:Ge_60s_Nr)

To make comparison of LIBS data with the SIMS data, the SIMS data results from the previous study on these samples [9], which are the ZnO:Ge non-reactive (Zn sputtered in the absence of O^- ions) samples of respectively annealed at 30s, 60s, 90s and remained as prepared. These samples were also produced exactly with the same process as the samples used in this study. Figure 4.8 to 4.11 showing the graphs of SIMS data accordingly;

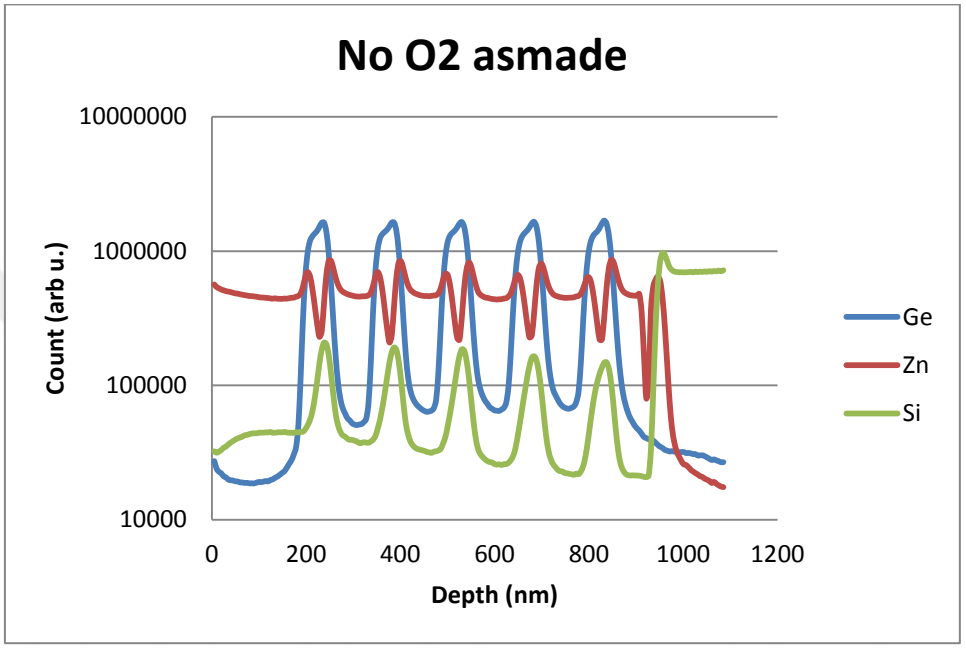

Figure 4.8 SIMS profile of ZnO:Ge_Nr_asmade

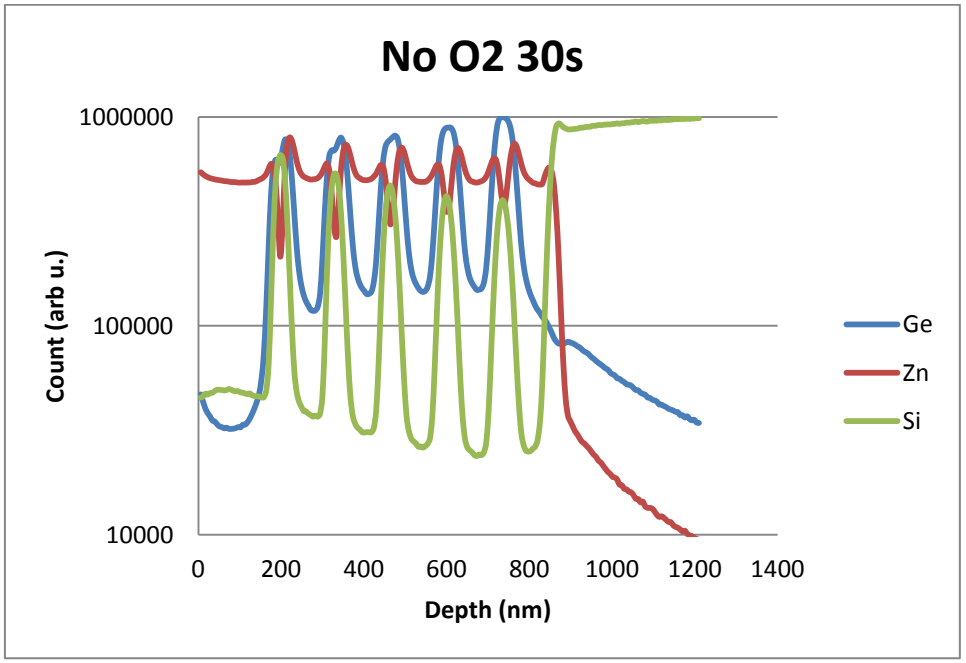

Figure 4.8 SIMS profile of ZnO:Ge_Nr_30s

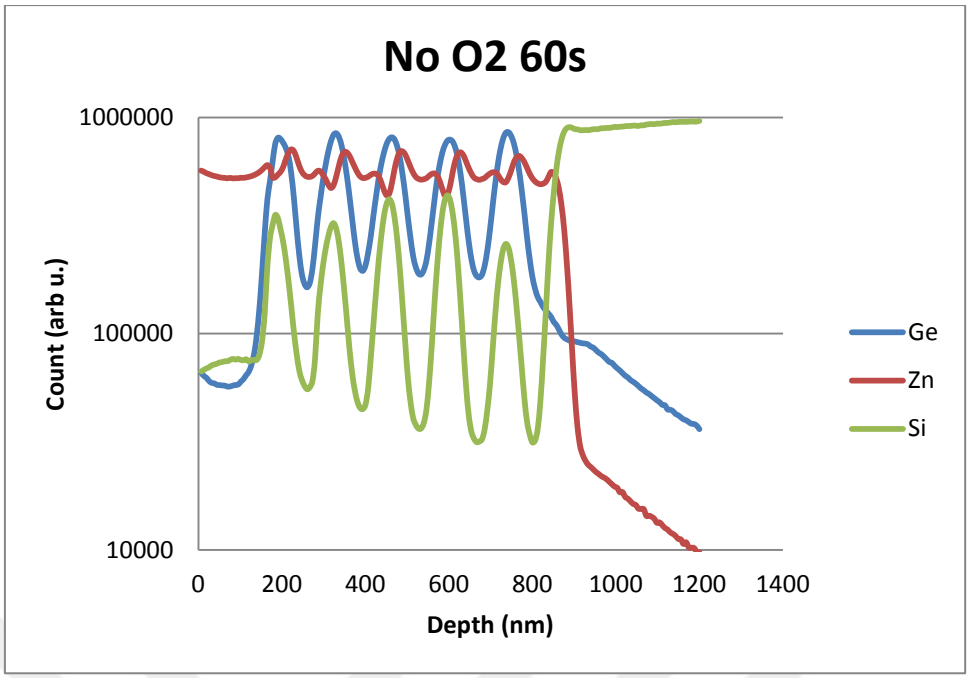

Figure 4.8 SIMS profile of ZnO:Ge_Nr_60s

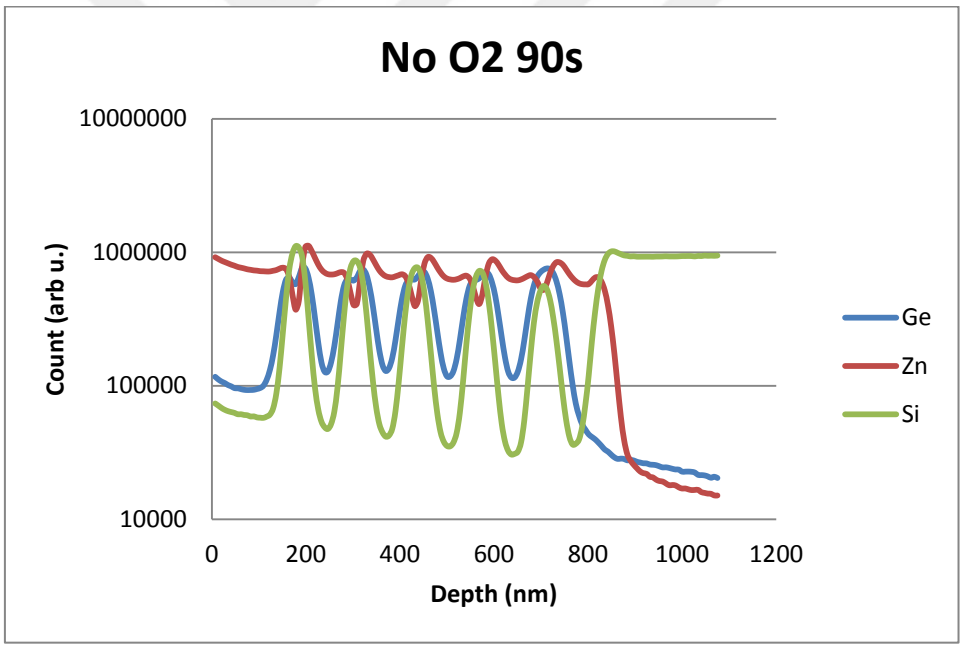

Figure 4.8 SIMS profile of ZnO:Ge_Nr_90s

When, one examines the data received from LIBS for depth profile in figure 3.8 to figure 3.11 especially for the Zn. It is obvious that after 10^{th} shot of laser pulse signal coming from Zn species is disappearing. If this information is combined with the data received from Dektak 150 Surface profiler, LIBS information is saying that with a approximately 125nm of single shot ablation depth, the thickness of the ZnO:Ge thin film is in a range of roughly 1,25 μm. At the same time SIMS graphs given above is so closely

proving the same film thickness with showing very week signal of Zn and Ge relatively after 1 μm.

The other compatible information from both structural analyses method is the information from Si component of the sample. If the Si spectrum signal is tracked from LIBS spectrum data, interestingly the substrate of the thin film composition could be observed from the very first shot, meaning that somehow Si atoms are present as well on the surface of the coating and even in between the Zn and Ge layers. SIMS signals for Si element is also giving the similar information and likely to prove the LIBS structural information for the sample.

Third point observed in this study is the homogeneity examination by LIBS, which is giving the results as; Location based homogeneity investigation for the sample ZnO:Ge_asmade is showing less fluctuations for Zn and Ge atoms location to location and shot to shot, meanwhile in the rest of the samples processed with different exposure times of RTA are heavily fluctuating by 1mm movement in the y-axis and in the consecutive shots. By looking at the SEM cross sectional images of the samples, at first glance it is seen that Ge and Zn formed as mostly linear layers, meanwhile the other samples processed with RTA is showing the Ge atoms segregate and crystallize as diamond cubic [25]. So the SEM images and the SIMS signals are likely to be aligned with the data obtained from LIBS.

5. Conclusion and Advises

As mentioned in the abstract of this study, it is tried to prove the LIBS as a promising method for fast and in-situ structural analyses for various kinds of thin film applications, especially developed and worked on to enhance the photo voltaic properties. It is well known that structural changes in the thin film formation may result with variations in the optical and electrical properties.

In nearly all methods of structure analyses, time needed to get the data and sample preparation process for the method used is long and inconvenient for urgent result needs for industrial applications of the thin films. On the other hand, LIBS method of structural analyses of such thin film applications still have to be enhanced and developed on the topics mentioned below which is an important outcome of this study;

Energy level of the laser source used in this study was not possible to go below 10mJ as because the detector used in this study is not capable to detect the spectral lines coming from Ge atoms in the sample. Increasing the energy level of the laser pulses are causing deep penetrations in the sample and lowering the measurement precision and measurement steps. This issue could be resolved by using ICCD instead of CCD detector in the future projects or the studies based on LIBS to increase the detection level of Ge atoms with the lower laser energies.

Due to lower transition probability of Ge atoms, it is not easy to distinguish the spectrum of the Ge from the other components of the samples investigated. LIBS method could give better results with different types of thin films that should be studied as a next step of this study.

Optical arrangement used in the study was planned as a common LIBS setup for solid sample measurements. This setup could be improved and developed with better optical focusing and expanding apparatus for the laser beam in order to get optimum spectral data from especially thin film samples in the further studies.

REFERENCES

[1] S. Cosentino, et al., The Role of The Surfaces In The Photon Absorption In Ge Nanoclusters Embedded In Slica, *Nanoscale Research Letters,* 6, 135 – 141, **2011**

[2] C. Uhrenfeldt, J. Chevallier, A.N. Larsen, B. Bech, Near-infrared-ultraviolet absorption cross-sections for Ge nanocrystals in SiO_2 thi fims: effect of shape and layer structure, *Journal Of Applied Physics,* 109, 094314-094327, **2011**

[3] D. Dawei, et al., Impacts of post metalisation process on the electrical and photovoltaic properties of Si quantum dot solar cells, *Nanoscale Research Letters,* 5, 1762-1767, **2010**

[4] M. Ficcadenti, et al., Si quantum dots for solar cell fabrication, *Material Science and Engineering,* B, 159-160, **2009**

[5] Y. Maeda, N. Tsukamoto, Y. Yazawa, Y. Masumoto, Visible photoluminescence of Ge microcrystals embedded in SiO_2 glassy matrices, *Applied Physics Letters,* 59, 3168 – 3170, **1991**

[6] A.G. Cullis, L.T. Canham, P.D. Calcott, The structural and luminescence properties of porous silicon, *Journal Of Applied Physics,* 82, 113126 – 113128, **1997**

[7] G.H. Shih, C.G. Allen, B.G. Potter Jr., Interfacial effects on the optical behavior of Ge:ITO and Ge:ZnO nanocomposite films, *Nanotechnology,* 23, 075203 – 075211, **2012**

[8] U. Pal, G.C. Segura, O.Z. Corona, Preparation of Ge/ZnO nanocomposites by radio frequency alternate sputtering, *Solar Energy Materials and Solar Cells,* 76, 305 – 312, **2003**

[9] Abdullah Ceylan, Ali E. Gümrükçü, Nihan Akın, Şadan Özcan, Süleyman Özçelik, Formation of ST12 Phase Ge nanoparticles in ZnO thin Films, *Material Scienci In Semiconductor Processing,* 40, 417 – 411, **2015**

[10] Şerife Yalçın , Sabiha Örer, Raşit Turan, 2-D analysis of Ge implanted SiO_2 surfaces by laser-induced breakdown spectroscopy, *Spectrochimica Acta Part B* 63, 1130-1138, **2008**

[11] W.R. Hindmarsh, Collision Broadening of spectral lines by neutral atoms, *Progress in Quantum Electronics*, 2, 143, **1973**

[12] D.D. Burgess, Spectroscopy of Laboratory Plasmas, *Space Science Review*, 13, 493, **1972**

[13] W.L. Kruer, The Physics of Laser Plasma Interaction, *Wesley*, New York, **1988**

[14] G. Bekefi, Principe of Laser Plasmas, *Wiley and Sons*, New York, **1976**

[15] D. A. Cremers, L, J. Radziemski, and T. R. Loree, Spectrochemical Analyses of Liquids Using the Laser Spark, *Applied Spectroscopy*, 38, 721, **1984**

[16] Svelto, O., *Principles of Laser,* 4th edition, Springer Berlin, **2004**

[17] Lorenzen, C. J., C. Carlhoff, U. Hahna and M. Jogwich, Application of Laser Induced Emission Spectral Analyses For Industrial Processes and Quality Control, *Journal Of Analytical Atomic Spectrometry,* 7, 1029-1035, **1992**

[18] Hecht, E., *Optics*, 4th edition, Addison-Wesley, **2001**

[19] D. F. Barbe, W. D. Baker, K. L. Davis, Signal Processing With Chargecoupled Devices, *Applied Physics,* 41, 91, **1979**

[20] Y. Maeda, N. Tsukamoto, Y. Yazawa, and Y. Masumoto, Visible photoluminesance of Ge microcrystals embedded in SiO2 glassy matrices, *Appl. Phys.Lett*, 59, 3168, **1991**

[21] A. G. Cullis, L. T. Canham, and P. D. Calcott, The Structural and Luminesance Properties of Porous Silicon, *Journal Applied Physics*, 82, 909, **1997**

[22] U. Pal, G. C. Segura, and O. Z. Corona, Preparation of Ge/ZnO Nanocomposites by Radio Frequency Alternate Sputtering, *Solar Energy Material Solar Cells*, 76, 306, **2003**

[23] S. D. Singh, R. S. Ajimsha, V. Sahu, R. Kumar, P. Misra, D. M. Phase, S. M. Oak, L. M. Kukreja, T. Ganguli, and S. K. Deb, Band Alignment and Interfacial Structure of ZnO/Ge heterojunction investigated by photoelectron spectroscopy, *Applied Physics Lett*, 101, 212109, **2012**

[24] T. Zheng, Z. Li, J. Chen, K. Shen, K. Sun, Transition of microstructure and photoluminescence of the Ge/ZnO multilayer films in certain annealing temperature region, *Applied Surface Science,* 252, 8482 – 8686, **2006**

[25] A. Ceylan, Abdul K. Rumaiz, Deniz Çalışkan, Şadan Özcan, Ekmel Özbay, Effects of Rapid Thermal Annealing On the Structural and Local Atomic Properties of ZnO:Ge nanocomposite thin films, *Journal Of Applied Physics,* 117, 105303, **201 5**

[26] U. Pal and J. G. Serrano, Raman and Infrared Spectroscopy of Ge Nanoparticles embedded in ZnO matrix, *Applied Surf. Science,* 246, 23, **2005**

[27] A. Ceylan, J. M. Ali, and S. Özcan, Synthesis of ZnO:Ge nanocomposite thin films by plasma gas condensation, *Material Science in Semiconductor Processing*, 16, 424, **2013**

[28] R. Wisburn, I. Schechter, R. Niesser, H. Schroder and K. I. Kompa, Analytic Chemistry, 66, 2964, **1994**

[29] J. D. Joannapoulus, M. L. Cohen, Electronic Properties of Complex Crystalline and Amorphous Phases of Ge and Si. I. Density of States and Band Structures, *Physics Rev.B,* 7, 2644 – 2657, **1973**

[30] S. Nozaki, S. Sato, S. Rath, H. Ono, H. Morisaki, Optical Properties of Tetragonal Germanium nanocrystals deposited by the clusted – beam evaporation technique: New light emmiting material for future, *Bull. Material, Science,* 22, 377-38, **1999**

[31] Eseller, K. E., *Laser Induced Incandescence And Laser Induced Breakdown Spectroscopy Based Sensor Development,* Doctor of Philosophy Thesis, Department of Physics and Astronomy, Mississippi, **2009**

[32] A.J. Miziolek, V. Palleschi, I. Schechter, *Laser Spectroscopy and Its Applications,* Marcel Dekker Inc., **1987**

[33] W. Demtroder, *Laser Spectroscopy Basic Concepts and Instrumentation,* Springer, **1996**

[34] J. P. Singh and S. N. Thakur, *Laser Induced Breakdown Spectroscopy,* Elsevier Science B. V., **2007**

[35] H.R. Griem, *Plasma Spectroscopy,* Mc Graw Hill, New York, **1964**

CURRICULUM VITAE

Credentials

Name, Surname : Mehmet Sinan Topcu

Place of Birth : Ankara

Marital Status : Married

E-mail : sinantopcu@gmail.com

Address : Ihlamur Cad. Ema Asmabahçe Konutları D Blok No: 20
Çayyolu / Ankara

Education

High School : TED Ankara Koleji (1992 – 1995)

Bsc : Hacettepe University Physics Engineering (1995 – 2000)

Foreign Language : English (Fluent)

Work Experience : Baxter Turkey Sağlık Hizmetleri (Technical Service Coordinator)

Areas of Experience : Medical devices

Projects and Budgets: -

Publications : -

Oral and Poster Presentations: -

HACETTEPE UNIVERSITY
GRADUATE SCHOOL OF SCIENCE AND ENGINEERING
THESIS/DISSERTATION ORIGINALITY REPORT

HACETTEPE UNIVERSITY
GRADUATE SCHOOL OF SCIENCE AND ENGINEERING
TO THE DEPARTMENT OF PHYSICS ENGINEERING

Date: 14/08/2016

Thesis Title / Topic: Structural analyses of Ge nanoparticles embedded ZnO thin films by

Laser Induced Breakdown Spectroscopy

According to the originality report obtained by ~~myself~~/my thesis advisor by using the *Turnitin* plagiarism detection software and by applying the filtering options stated below on 14/08/2016 for the total of 70 pages including the a) Title Page, b) Introduction, c) Main Chapters, and d) Conclusion sections of my thesis entitled as above, the similarity index of my thesis is 8 %.

Filtering options applied:

1. Bibliography/Works Cited excluded
2. Quotes excluded
3. Match size up to 5 words excluded

I declare that I have carefully read Hacettepe University Graduate School of Sciene and Engineering Guidelines for Obtaining and Using Thesis Originality Reports; that according to the maximum similarity index values specified in the Guidelines, my thesis does not include any form of plagiarism; that in any future detection of possible infringement of the regulations I accept all legal responsibility; and that all the information I have provided is correct to the best of my knowledge.

I respectfully submit this for approval.

14.08.2016
Date and Signature

Name Surname:	Mehmet Sinan TOPCU
Student No:	N14227526
Department:	Physics Engineering
Program:	Physics Engineering
Status:	☒ Masters ☐ Ph.D. ☐ Integrated Ph.D.

ADVISOR APPROVAL

APPROVED.

Assoc.Prof.Dr. Abdullah CEYLAN

(Title, Name Surname, Signature)